Original research

Patients with mesenchymal tumours and high *Fusobacteriales* prevalence have worse prognosis in colorectal cancer (CRC)

Manuela Salvucci ,[1] Nyree Crawford,[2] Katie Stott,[2] Susan Bullman,[3] Daniel B Longley,[2] Jochen H M Prehn[1]

► Additional supplemental material is published online only. To view, please visit the journal online (http://dx.doi.org/10.1136/gutjnl-2021-325193).

[1]Centre for Systems Medicine, Department of Physiology and Medical Physics, Royal College of Surgeons in Ireland, Dublin, Ireland
[2]Patrick G Johnston Centre for Cancer Research, School of Medicine, Dentistry and Biomedical Science, Queen's University Belfast, Belfast, UK
[3]Human Biology, Fred Hutchinson Cancer Research Center, Seattle, Washington, USA

Correspondence to
Professor Jochen H M Prehn, Department of Physiology and Medical Physics and Centre for Systems Medicine, Royal College of Surgeons in Ireland, Dublin, Ireland; jprehn@rcsi.ie

Received 18 May 2021
Accepted 31 August 2021
Published Online First
8 September 2021

To cite: Salvucci M, Crawford N, Stott K, *et al*. *Gut* 2022;**71**:1600–1612.

ABSTRACT

Objectives Transcriptomic-based subtyping, consensus molecular subtyping (CMS) and colorectal cancer intrinsic subtyping (CRIS) identify a patient subpopulation with mesenchymal traits (CMS4/CRIS-B) and poorer outcome. Here, we investigated the relationship between prevalence of *Fusobacterium nucleatum* (*Fn*) and *Fusobacteriales*, CMS/CRIS subtyping, cell type composition, immune infiltrates and host contexture to refine patient stratification and to identify druggable context-specific vulnerabilities.

Design We coupled cell culture experiments with characterisation of *Fn*/*Fusobacteriales* prevalence and host biology/microenviroment in tumours from two independent colorectal cancer patient cohorts (Taxonomy: n=140, colon and rectal cases of The Cancer Genome Atlas (TCGA-COAD-READ) cohort: n=605).

Results In vitro, *Fn* infection induced inflammation via nuclear factor kappa-light-chain-enhancer of activated B cells/tumour necrosis factor alpha in HCT116 and HT29 cancer cell lines. In patients, high *Fn*/*Fusobacteriales* were found in CMS1, microsatellite unstable () tumours, with infiltration of M1 macrophages, reduced M2 macrophages, and high interleukin (IL)-6/IL-8/IL-1β signalling. Analysis of the Taxonomy cohort suggested that *Fn* was prognostic for CMS4/CRIS-B patients, despite having lower *Fn* load than CMS1 patients. In the TCGA-COAD-READ cohort, we likewise identified a differential association between *Fusobacteriales* relative abundance and outcome when stratifying patients in mesenchymal (either CMS4 and/or CRIS-B) versus non-mesenchymal (neither CMS4 nor CRIS-B). Patients with mesenchymal tumours and high *Fusobacteriales* had approximately twofold higher risk of worse outcome. These associations were null in non-mesenchymal patients. Modelling the three-way association between *Fusobacteriales* prevalence, molecular subtyping and host contexture with logistic models with an interaction term disentangled the pathogen–host signalling relationship and identified aberrations (including NOTCH, CSF1-3 and IL-6/IL-8) as candidate targets.

Conclusion This study identifies CMS4/CRIS-B patients with high *Fn*/*Fusobacteriales* prevalence as a high-risk subpopulation that may benefit from therapeutics targeting mesenchymal biology.

Significance of this study

What is already known on this subject?

⇒ *Fusobacterium nucleatum* (*Fn*), a commensal Gram-negative anaerobe from the *Fusobacteriales* order, is an oncobacterium in colorectal cancer (CRC), and a causal relationship between *Fn* prevalence and CRC pathogenesis, progression and treatment response has been reported in vivo.

⇒ Broad-spectrum antibiotics have proven moderately successful in reducing tumour growth promoted by *Fn* in preclinical models. However, the use of antibiotics to treat bacterium-positive cases in the clinic is not a viable option as it may further alter the already dysbiotic gut microbiome of patients with CRC and may also have limited efficacy against *Fn*, which penetrates and embeds deeply within the tumour.

⇒ The highly heterogeneous population of patients with CRC can be classified into distinct molecular subtypes (consensus molecular subtyping (CMS) and colorectal cancer intrinsic subtyping (CRIS)) based on gene expression profiles mirroring the underlying transcriptional programmes. Patients classified as CMS4 and CRIS-B exhibit a mesenchymal phenotype and have poorer outcome.

INTRODUCTION

Colorectal cancer (CRC) has one of the highest morbidities and mortality rates among solid cancers, and its incidence is steadily on the rise, accounting for circa 10% of newly diagnosed cancer cases worldwide.[1] Patients with CRC with similar macroscopic clinicopathological characteristics exhibit a high degree of heterogeneity at the molecular level, which translates into heterogeneous and often suboptimal response to treatment. Thus, research has focused on molecular subtyping strategies based on single or multiomics data from the host to categorise patients into subgroups to aid in risk stratification and disease management. Subtyping strategies such as the consensus molecular subtyping (CMS[2]) and the colorectal cancer intrinsic subtyping (CRIS[3]) classify patients into subgroups with more homogeneous signalling features based on key transcriptomic programmes. Among the four subtypes identified by the CMS classifier, CMS4 patients have high stroma infiltration along with upregulated angiogenesis and transforming growth

Significance of this study

What are the new findings?

⇒ *Fn*/*Fusobacteriales* prevalence is associated with immune involvement (decrease in antitumour M1 macrophages and increase in protumour M2 macrophages) and activation of specific signalling programmes (inflammation, DNA damage, WNT, metastasis, proliferation and cell cycle) in the host–tumours.

⇒ The prevalence of bacteria from the *Fusobacteriales* order, largely driven by *Fn* species, plays an active or opportunistic role, depending on the underlying host–tumour biology and microenvironment.

⇒ *Fn* and other species of the *Fusobacteriales* order are enriched in CMS1 (immune-high, microsatellite unstable tumours) patients compared with CMS2–4 cases.

⇒ *Fn*/*Fusobacteriales* prevalence is associated with worse clinical outcome in patients with mesenchymal-rich CMS4/CRIS-B tumours but not in patients with other molecular subtypes.

How might it impact on clinical practice in the foreseeable future?

⇒ *Fn*/*Fusobacteriales* screening and transcriptomic-based molecular subtyping should be considered to identify patients with mesenchymal-rich tumours and high bacterium prevalence to inform disease management.

⇒ *Fn*/*Fusobacteriales* prevalence may need to be addressed exclusively in patients with mesenchymal-rich high-stromal infiltrating tumours rather than a blanket approach to treat all pathogen-positive patients.

⇒ Clinical management of the disease for this subpopulation of high-risk patients with unfavourable clinical outcome could be attained by administering agents currently in clinical trials that target aberrations in the host signalling pathways (NOTCH, WNT and epithelial-mesenchymal transition) and tumour microenviroment (inflammasome, activated T cells, complement system, and macrophage chemotaxis and activation).

factor-β (TGF-β) signalling and show poorer recurrence-free and overall survival.[2] Similarly, CRIS-B patients feature mesenchymal traits and also exhibit poorer outcome compared with patients classified as CRIS-A and CRIS-C–E.[3]

Recent research has identified the microbiome as a key player in health and disease, including cancer.[4] Several research groups, including ours, have shown that *Fusobacteriales*, largely from *Fusobacterium nucleatum* (*Fn*), are more abundant in tumour tissue compared with matched adjacent mucosa,[5] suggesting a causative role in CRC progression.[6] More advanced, right-sided, MSI tumours are typically enriched with *Fn*.[7] Remarkably, antimicrobial treatment has been shown to reduce tumour burden in mouse xenograft models,[8] corroborating the association between *Fn*-positive patients and poorer outcome observed in some studies.[5] However, the prognostic value of *Fn* prevalence was not observed in other cohort studies (reviewed in Gethings-Behncke *et al*[9]). Thus, we hypothesised that the impact of *Fn*/*Fusobacteriales* may differ according to the underlying tumour biology.

In this study, we combined mechanistic in vitro experiments in colon cancer cells with an in-depth analysis in two independent CRC patient cohorts and a systematic multi*omic* characterisation of cell signalling and tumour microenvironment in n=745 patients to investigate the interaction between the dysregulation induced by *Fusobacteriales* prevalence (including *Fn*) on the human host and, conversely, the characteristics of the host microenvironment that allow pathogens to thrive. Here, we provide evidence that the prognostic value of *Fn*/*Fusobacteriales* strongly relates to the molecular subtype of the host–tumour and is confined to subtypes showing mesenchymal involvement.

MATERIALS AND METHODS

Detailed methods for the in vitro experiments and the patients' study (design, cohorts' description and analysis steps) are provided in the online supplemental materials and methods.

RESULTS

Fn infection induces inflammation mediated by tumour necrosis factor alpha (TNF-α) and NFκB in CRC cellular cultures

Due to the presence of *Fn* in CRC tumour tissue,[5 8] a causative role for this bacterium in exacerbating tumourigenesis has been put forward. Infection of colon cells with *Fn* has previously been shown to induce inflammation, activate NFκB signalling and increase expression of the proinflammatory cytokine TNF-α[10 11] (figure 1A). Hence, we infected HCT116 and HT29 colon cancer cell line cultures for 6 hours to assess epithelial cell response to increasing amounts of *Fn* (multiplicity of infection, (MOI), bacteria-to-cancer-cells: 10, 100 and 1000). We found that NFκB signalling was activated on infection with *Fn* in CRC cell lines, as evidenced by the degradation of IκBα (alpha nuclear factor of kappa light polypeptide gene enhancer in B-cell inhibitor) (figure 1B), an increase in NFκB transcriptional activity (figure 1C) and a marked increase in mRNA expression of the NFκB target gene, TNF-α (figure 1D). Taken together, these results confirm that *Fn* coculture with human colon cancer epithelial cells promotes a proinflammatory response.

Prevalence of *Fn*/*Fusobacteriales* in tumour resections

We sought to investigate the relationship between inflammation in the human host and prevalence of *Fn* and *Fusobacteriales* in tumour resections of patients with CRC. We selected an in-house multicentre stage II–III cohort (Taxonomy, n=140[12 13]) and the colon and rectal cases of The Cancer Genome Atlas (TCGA-COAD-READ cohort, n=605 patients; figure 2A) to encompass the heterogeneity of the CRC clinicopathological characteristics observed in the clinic. Demographic, clinicopathological characteristics for the Taxonomy and TCGA-COAD-READ cohorts are summarised in online supplemental table 1. We determined *Fn* load by a targeted quantitative real-time PCR in tumour resections of the Taxonomy cohort where we detected *Fn* in n=101 of 140 (72%) patients (figure 2B and online supplemental table 2). The distribution of *Fn* positivity levels (relative to the human PGT gene) was heterogeneous, and we categorised patients as *Fn*-high or *Fn*-low using the 75th percentile as cut-off (figure 2B). We estimated *Fusobacteriales* relative abundance (RA) in the TCGA-COAD-READ cohort from RNA sequencing data by mapping non-human reads to microbial reference databases and retaining only high-quality matches (see the Materials and methods section) with a *PathSeq* analysis[14 15] (figure 2A and online supplemental table 2). For downstream analyses, we reported the RA at the order, family, genus and species taxonomic rank, and expressed it as percentage of the

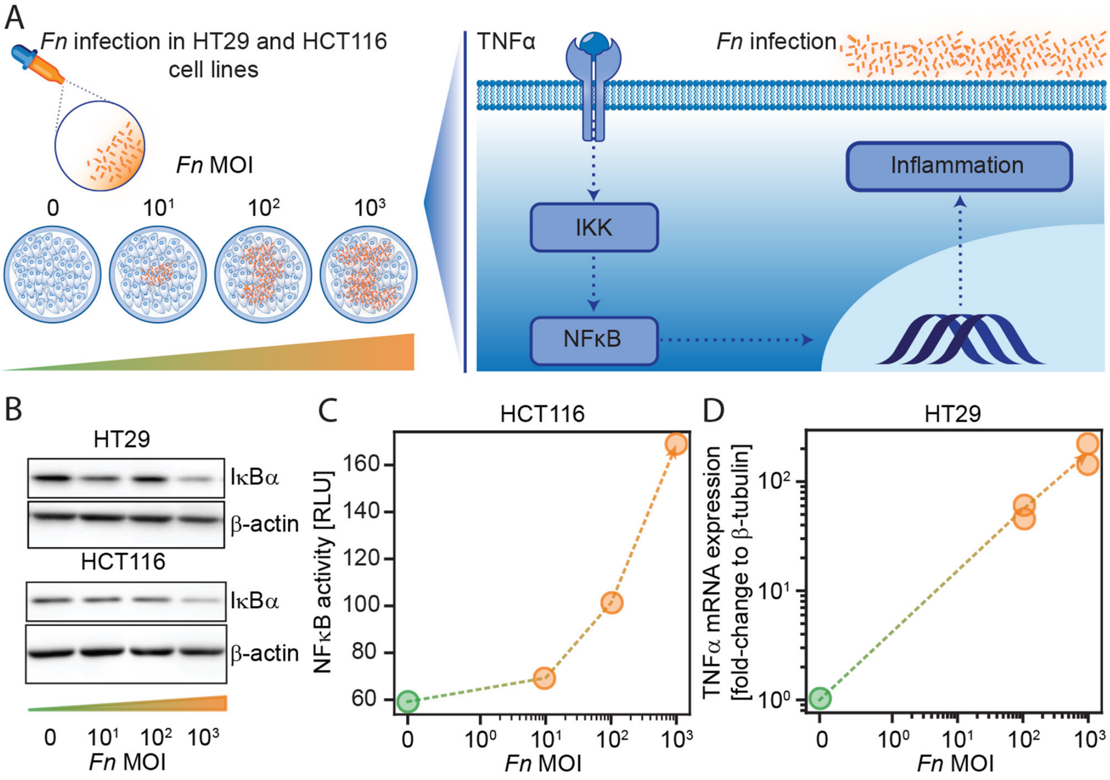

Figure 1 *Fn* infection induces inflammation mediated by TNF-α and NFκB in HCT116 and HT29 CRC cell lines. (A) Schematic representation of the experimental set-up to investigate how *Fn* may trigger inflammation via TNF-α and NFκB signalling pathways. (B) Western blot analysis of IκBα and β-actin in HT29 and HCT116 cell cultures following infection with *Fn* (MOI bacteria-to-cancer-cells 10, 100 and 1000). (C) NFκB transcriptional activity assay in HCT116 cells 6 hours following infection with *Fn* (MOI bacteria-to-cancer-cells 100 and 1000). (D) TNF-α mRNA expression relative to β-tubulin in HT29 cells 6 hours following infection with *Fn* (MOI bacteria-to-cancer-cells 100 and 1000). (B–D) Representative results from duplicate experiments. *Fn*, *Fusobacterium nucleatum*; TNF-α, tumour necrosis factor alpha.

total bacterial abundance. We detected *Fusobacteriales* (defined as RA over zero, at the order level) in n=558 of 605 (92%) of the TCGA-COAD-READ patients (figure 2D). *Fn* was the most abundant species and was detected in 82% of the TCGA-COAD-READ patients (compared with 72% in the Taxonomy cohort), accounting on average for approximately 45% of total *Fusobacteriales* RA and accounting for over 75% of total *Fusobacteriales* RA in 16% of cases (figure 2C). Analogous to the Taxonomy cohort, we categorised patients as *Fusobacteriales*-high or *Fusobacteriales*-low using the 75th percentile as cut-off.

Higher *Fn*/*Fusobacteriales* prevalence correlates with inflammation and immune involvement

We examined the association between host gene expression profiles of key inflammatory markers and either *Fn* load or *Fusobacteriales* RA in the Taxonomy and TCGA-COAD-READ cohorts, respectively. In line with the in vitro experiments (figure 1), we detected an increase in NFKB1 and a trend in TNF-α gene expression, recapitulated by transcriptomic-based signatures for an overall inflammation status mediated by the cytolytic and interferon gamma (IFN-γ) pathways in the Taxonomy cohort (figure 2E). When investigating further key inflammation players, we observed a marked increase in proinflammatory interleukins (ILs) (IL-6, IL-8, IL-10, IL-1β and IL-13), cytokines/chemokines (CCL8, CSF1 and ICAM1), metalloproteins (MMP1, MMP3 and MMP9), NOS2, the inflammasome complex (NLRP3) and decrease in COX2 in *Fn*-high versus *Fn*-low Taxonomy patients (figure 2E and online supplemental figure 1).

We sought to validate and build on our findings from the in-house Taxonomy cohort by analysing the TCGA-COAD-READ cohort (figure 2F). At the transcription level, we confirmed an exacerbated inflammatory state when comparing *Fusobacteriales*-high and *Fusobacteriales*-low patients mediated by the NFκB–TNF-α axis and IFN-γ with cytolytic involvement. *Fusobacteriales*-high patients overexpressed proinflammatory ILs (IL-6, IL-8, IL-10 and IL-1β), cytokines/chemokines (CCL8 and ICAM1), metalloproteinases (MMP1 and MMP3), NOS2 and inflammasome markers (NLRP3) (figure 2F).

As inflammation is strongly tied to immune cell migration and activity, we investigated whether there was a link between immune cell composition and either *Fn* load (taxonomy) or *Fusobacteriales* RA (TCGA-COAD-READ). Cell composition was computationally deconvoluted from gene expression profiles with quanTiseq[16] and microenvironment cell populations (MCP)-counter[17] (figure 2G,H). Despite observing high interpatient heterogeneity in cell composition within the Taxonomy and TCGA-COAD-READ cohorts, we detected higher immune cell activation and polarisation when comparing patients with high versus low *Fn* load (Taxonomy) or *Fusobacteriales* RA (TCGA-COAD-READ). Patients with high *Fn* load (Taxonomy) or *Fusobacteriales* (TCGA-COAD-READ) showed higher predicted abundance of regulatory T cells coupled with an increase in M1 macrophages and a decrease in M2 macrophages (figure 2I,J). MCP-counter identified a strong positive association between neutrophil infiltration and either *Fn* load (Taxonomy) or *Fusobacteriales* RA (TCGA-COAD-READ). However, no difference in predicted neutrophils abundance was detected by quanTIseq.

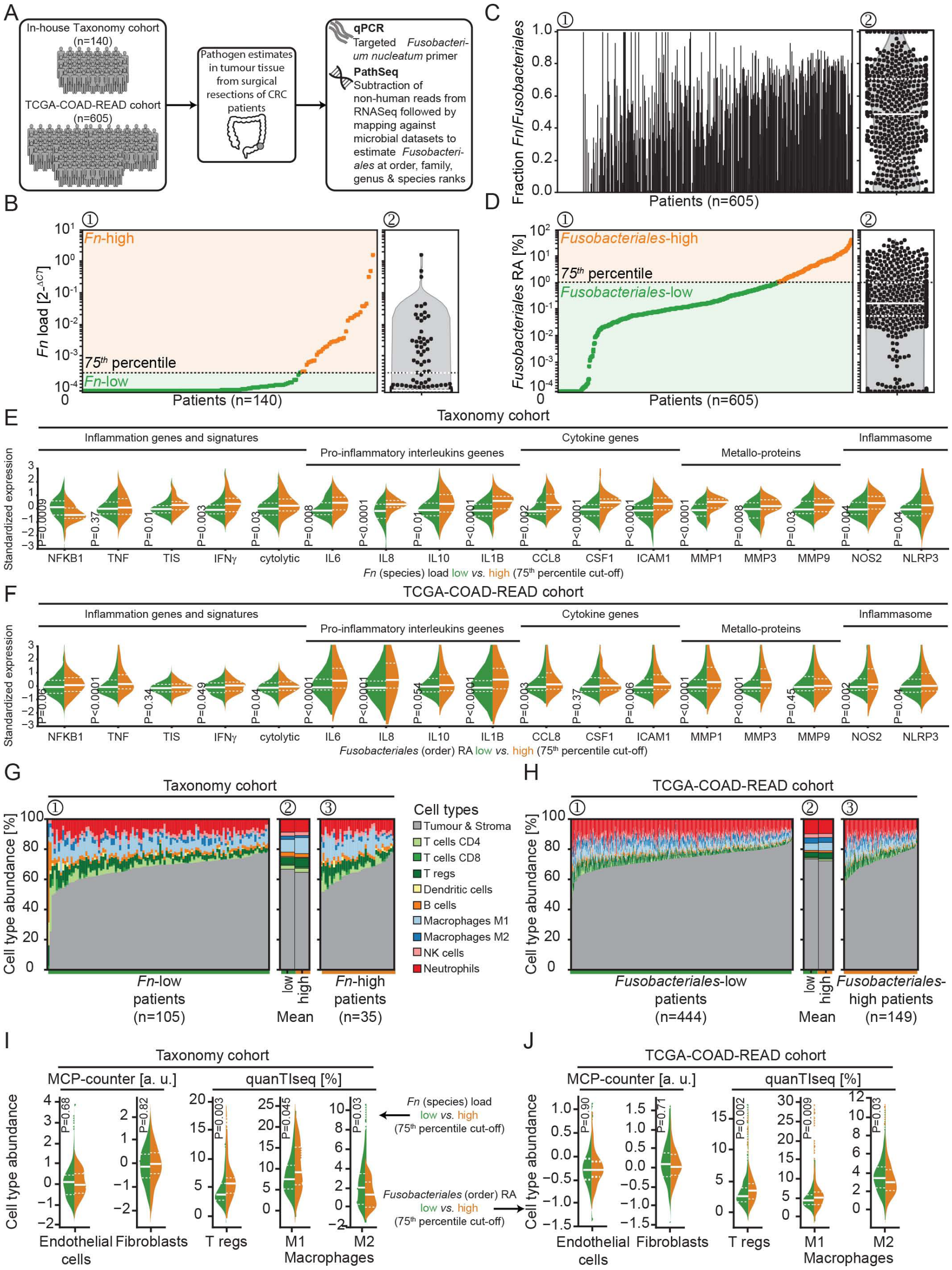

Figure 2 *Fn*/*Fusobacteriales* prevalence is associated with inflammation and immunosuppression in patients with CRC of the Taxonomy and TCGA-COAD-READ CRC cohorts. (A) Schematic representation of the cohorts included in the study and methods to estimate *Fn* load and *Fusobacteriales* (order) RA in the Taxonomy and TCGA-COAD-READ cohorts, respectively. (B–D) Per-patient (waterfall plot, 1, left) and distribution (violin plot with overlaid data-points, 2, right) of bacterium prevalence in tumour resections of the Taxonomy (n=140, B) and TCGA-COAD-READ (n=605, D). In B,D 1, patients are sorted in ascending order of either *Fn* load (Taxonomy cohort, B) or *Fusobacteriales* RA at the order taxonomic rank (TCGA-COAD-READ cohort, D). Cut-off of 75th percentile used for patients' stratification in downstream analysis is also indicated (black dotted line). (C) Corresponding per-patient fraction of *Fn* species to total *Fusobacteriales* order RA detected for the TCGA-COAD-READ cohort . (E,F) Violin plots depicting the expression distribution of key genes or signatures involved in inflammation and immunosuppression grouped by patients with low (in green) or high (in orange) either *Fn* load (Taxonomy cohort, E) or *Fusobacteriales* RA at the order taxonomic rank (TCGA-COAD-READ cohort, F). Median and lower (25th) and upper (75th) percentiles are indicated by white solid or dashed lines, respectively. Statistical significance was evaluated using Kruskal-Wallis tests and p values are reported. (G,H) Stacked bar plots indicating cell type composition per patient estimated from gene expression by quanTIseq in tumours with low versus high either *Fn* load (Taxonomy cohort, G) or *Fusobacteriales* RA at the order taxonomic rank (TCGA-COAD-cohort, H). Cell type composition is shown sorted in ascending order of tumour and stromal content (1 and 3) and aggregated (by mean, 2 across the low and high subgroups). (I,J) Distribution of specific tumour/stroma and immune cell types determined as indicated by either quanTIseq or MCP-counter grouped by either *Fn* load (Taxonomy cohort, I) or *Fusobacteriales* RA at the order taxonomic rank (TCGA-COAD-READ cohort, J). Median and lower (25th) and upper (75th) percentiles are indicated by white solid or dashed lines, respectively. Statistical significance was evaluated using Kruskal-Wallis tests and p values are reported. CRC, colorectal cancer; *Fn*, *Fusobacterium nucleatum*; NK, natural killer cells; RA, relative abundance; TCGA-COAD-READ, colon and rectal cases of The Cancer Genome Atlas; Treg, regulatory T cell.

Importantly, no difference in fibroblasts and endothelial cells was observed by *Fn/Fusobacteriales* in either cohort by either method (figure 2I,J).

Multiomic characterisation of the association between *Fusobacteriales* RA and human host–tumour microenvironment in the TCGA-COAD-READ cohort

We leveraged the rich molecular characterisation of the TCGA-COAD-READ cohort to perform a systematic and unbiased characterisation of the association between *Fusobacteriales* RA and patient clinical and molecular features to identify human host vulnerabilities that may be conducive for tumour development (figure 3).

We observed higher *Fusobacteriales* in patients of older age, diagnosed with more advanced disease stage and tumours located in the colon, particularly in proximal site (figure 3A) cohorts. In contrast, we found no statistically significant differences in *Fusobacteriales* RA by sex, body mass index and either lymphovascular or perineural invasion (online supplemental figure 2). We observed similar patterns and a slightly higher prevalence in women (Taxonomy cohort, p=0.049), when assessing *Fn* in both the TCGA-COAD-READ and Taxonomy cohorts (online supplemental figure 3A), corroborating previous studies.[18]

Patients harbouring higher *Fusobacteriales* showed lower genomic intratumour heterogeneity, had higher silent and non-silent mutational burden and were enriched in microsatellite unstable cases (figure 3B and online supplemental figure 3B). *Fusobacteriales*-high patients had an increase in transitions, defined as the exchange of two-ring purines (A↔G) or of a one-ring pyrimidines (C↔T), coupled with a decrease in transversions, a substitution of purine for pyrimidine bases (online supplemental figure 4A) as evidenced by a decrease in conversion changes of C>G and T>A (online supplemental figure 4B). We found no difference in prevalence of common mutations in CRC by *Fusobacteriales* (low vs high) except for *BRAF* (figure 3C). *BRAF* mutations trended to be more common among *Fusobacteriales*-high and *Fn*-high patients, as previously reported when assessing *Fn*[18] (figure 3C and online supplemental figure 3B). A comprehensive screen revealed that mutations in cell cycle (ATM), Hedgehog signalling (MEGF8), DNA damage/repair (TRIP12 and PRKDC), mitotic spindle (ASPM) and migration/adhesion (TRIO, GPR98) were more prevalent in *Fusobacteriales*-high patients (figure 3D) (online supplemental table 3).

We set out to investigate the relationship between copy number alterations (CNAs) and *Fusobacteriales* presence in the TCGA-COAD-READ cohort (figure 3E–G). We determined recurrent CNA amplifications and deletions across the whole cohort by applying the genomic identification of significant targets in cancer (GISTIC) algorithm[19] (online supplemental figures 5 and 6 and online supplemental table 4). *Fusobacteriales*-high cases showed lower chromosomal instability with a lower fraction of the genome affected by recurrent CNAs, in line with the increased incidence of MSI. We identified CNA amplifications or deletions, the frequency of occurrence of which differed between *Fusobacteriales*-high versus *Fusobacteriales*-low patients and, thus, may be specifically associated with the bacterium presence (figure 3F). CNAs more frequently (>15%) observed in *Fusobacteriales*-high versus *Fusobacteriales*-low cases included deletions in 8p23.2 (tumour suppressor CSMD1 and LOC100287015), 18q21.1 (MIR4743 and RNA binding by CTIF) and 18q23, which impact the regulation of IL-6 and chemokine secretion, cell–cell adhesion and host response of viral transcription (figure 3G).

We then focused on the transcriptional level and combined enrichment analyses with pathway-activity signatures to compare the impact of *Fusobacteriales* RA on cellular processes (figure 3H–J). Transcriptional profiles that differed included mTORC1 and cMYC signalling, cell cycle (G2-M checkpoint), mitotic spindle, epithelial-to-mesenchymal transition, TGF-β and IL-1 regulation of extracellular matrix, matrix remodelling including focal adhesion, cytoskeleton and contractile actin filament bundle, mitochondrial translational elongation/termination, and protein complex assembly and stromal estimates (figure 3H,I, online supplemental figure 7 and supplemental table 5). We corroborated these findings by comparing the activation of signalling pathways estimated by gene set signatures identified in the literature (see the Materials and methods section) in *Fusobacteriales*-low versus *Fusobacteriales*-high patients. *Fusobacteriales* RA was inversely linked to WNT signalling and positively associated with proliferation, metastasis (figure 3J) and DNA damage.

We sought to investigate whether the findings at the genomic and transcriptional levels were also observed in protein profiles determined by reverse phase protein array. We found that *Fusobacteriales* RA correlated with differential expression of proteins involved in microenvironment composition (Claudin7), cell cycle (Cyclin1), cMYC, apoptosis (cleaved Caspase7), proliferation (DLV3), Hippo pathway (Yap), DNA damage (Chk1 and ATM), receptor and mitogen-activated protein(MAP) kinases and PI3K signalling (figure 3K–M, online supplemental figure 8 and supplemental table 6).

Fn/*Fusobacteriales* prevalence differs by transcriptomic-based molecular subtype

The aforementioned systematic screen pinpointed host aberrations associated with *Fusobacteriales* hallmarked by transcriptomics-based molecular subtypes. Hence, we classified patients in the study by CMS[2] and CRIS[3] subtyping. We observed higher *Fn* load (Taxonomy, figure 4A) and *Fusobacteriales* RA (TCGA-COAD-READ, figure 4C) in immune-high CMS1 tumours, corroborating the link between pathogen prevalence and host immunity. We observed higher *Fn* load in CRIS-B tumours (figure 4B) and *Fusobacteriales* RA in CRIS-A cases (figure 4D) of the Taxonomy and TCGA-COAD-READ cohorts, respectively. At the family rank, *Fusobacteriaceae* were more abundant than *Leptotrichiaceae*, accounting for 77% and 23% of total *Fusobacteriales* RA and ~2% and ~<1% of the total bacteria RA, respectively. In line with the findings at the order level, we observed an increase in *Fn*, the most abundant *Fusobacterium* species, in CMS1 and CRIS-A cases (figure 4E,F). In line with the findings at the order level, we observed an approximately threefold increase when comparing patients classified as CMS1 versus the rest (figure 4E). *Fn*, the most abundant *Fusobacterium* species, was enriched in CMS1 and CRIS-A cases (figure 4E,F). We examined whether the positive association between inflammation and immune involvement by *Fn*/*Fusobacteriales* presence could be ascribed to the host CMS1 milieu or whether there was an additional pathogen-induced component. When restricting the analysis to CMS1 cases, we observed higher expression of proinflammatory markers in *Fusobacteriales*-high patients of the TCGA-COAD-READ cohort. We detected no association between pathogen prevalence and expression of anti-inflammatory markers or inflammation signatures in either CRC cohort (figure 4G,H). Taken together, these results suggest that

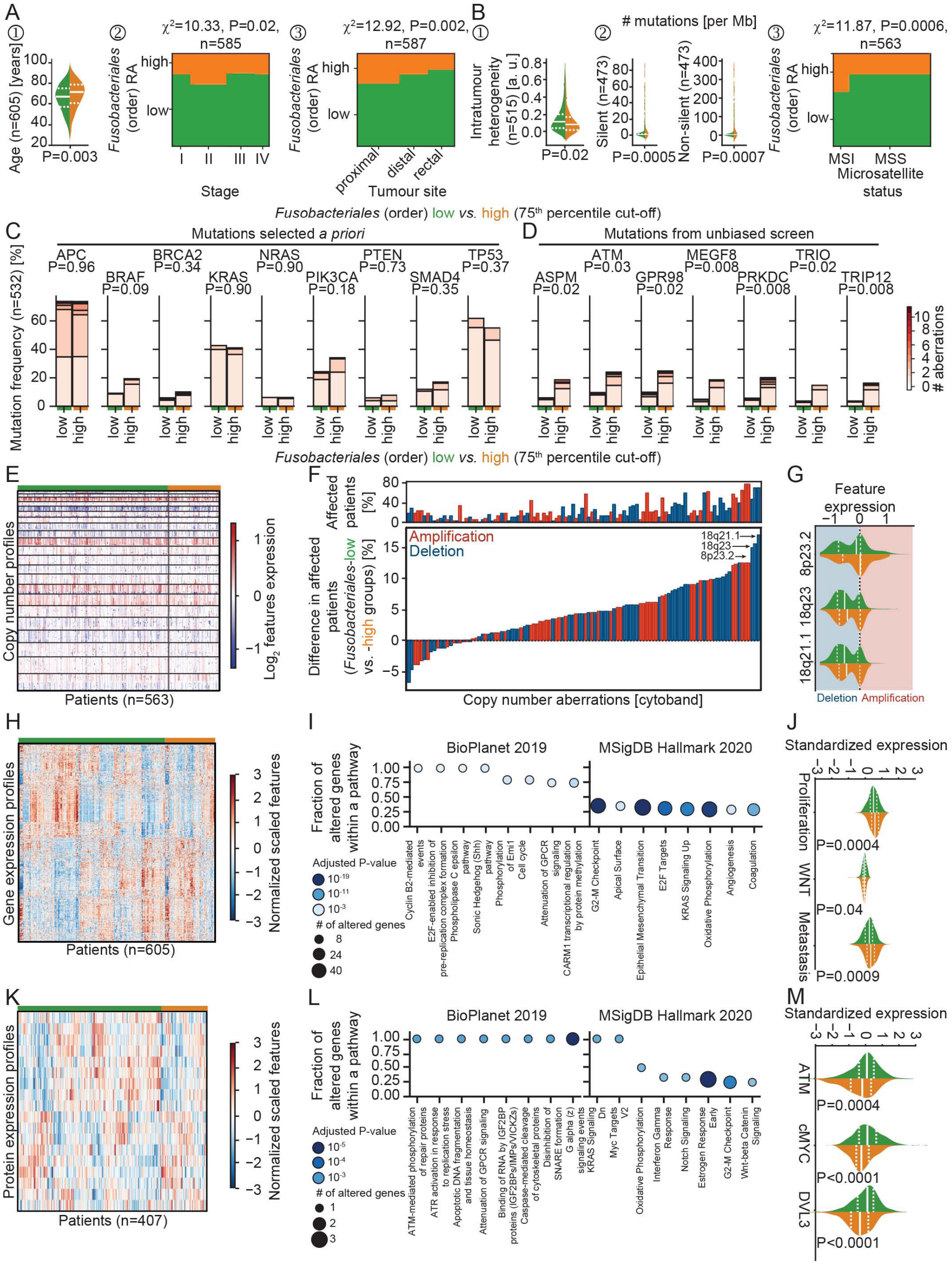

Figure 3 Multiomic characterisation of the association between *Fusobacteriales* RA and human host–tumour microenvironment in the TCGA-COAD-READ cohort. (A,B). Association between *Fusobacteriales* at the order taxonomic rank binned into low versus high (cut-off 75th percentile) and clinicopathological (A) and mutational (B) characteristics of the human host. (C,D) Comparison of frequency of occurrence of mutations selected a priori (C) or identified by an unbiased scan (D) in *Fusobacteriales*-low versus *Fusobacteriales*-high patients. Colour bar indicates number of detected aberrations among frame shift deletions and insertions, in frame deletions and insertions, missense and nonsense mutations, and splice sites. P values were computed with χ^2 independence tests and adjusted for multiple comparisons (Benjamini-Hochberg false discovery rate). (E–G) Heatmap (E) displaying copy number alterations grouped by *Fusobacteriales*-low (in green) and *Fusobacteriales*-high (in orange) RA. Waterfall plot (F) displaying differences in recurrent copy number aberrations detected in patients with low *Fusobacteriales* versus high *Fusobacteriales*. Top panel (F) reports percentage of patients affected by recurrent copy number aberrations. Distribution of top 3 deletions, the frequency of occurrence of which differs between *Fusobacteriales*-low and *Fusobacteriales*-high patients (G). Red and blue shadings indicate amplification and deletions, respectively. (H–J) Heatmap (H) displaying expression of genes differentially expressed when comparing *Fusobacteriales*-low versus *Fusobacteriales*-high patients and corresponding pathway enrichment analysis (I). Expression distribution grouped by *Fusobacteriales* RA (low, in green, vs high, in orange) for selected gene expression signatures (J). (K–M) Heatmap (K) displaying expression of proteins differentially expressed when comparing *Fusobacteriales*-low versus *Fusobacteriales*-high patients and corresponding pathway enrichment analysis (L). Expression distribution grouped by *Fusobacteriales* RA (low, in green, vs high, in orange) for key proteins (M). In violin plots, the median and lower (25th) and upper (75th) percentiles are indicated by white solid or dashed lines, respectively. Green and orange annotation bars denote patients with low versus high *Fusobacteriales* RA (75th percentile cut-off). (Unadjusted) P values (J,M) were determined by Kruskal-Wallis tests. MSS, patients with microsatellite stable tumours; RA, relative abundance; TCGA-COAD-READ, colon and rectal cases of The Cancer Genome Atlas.

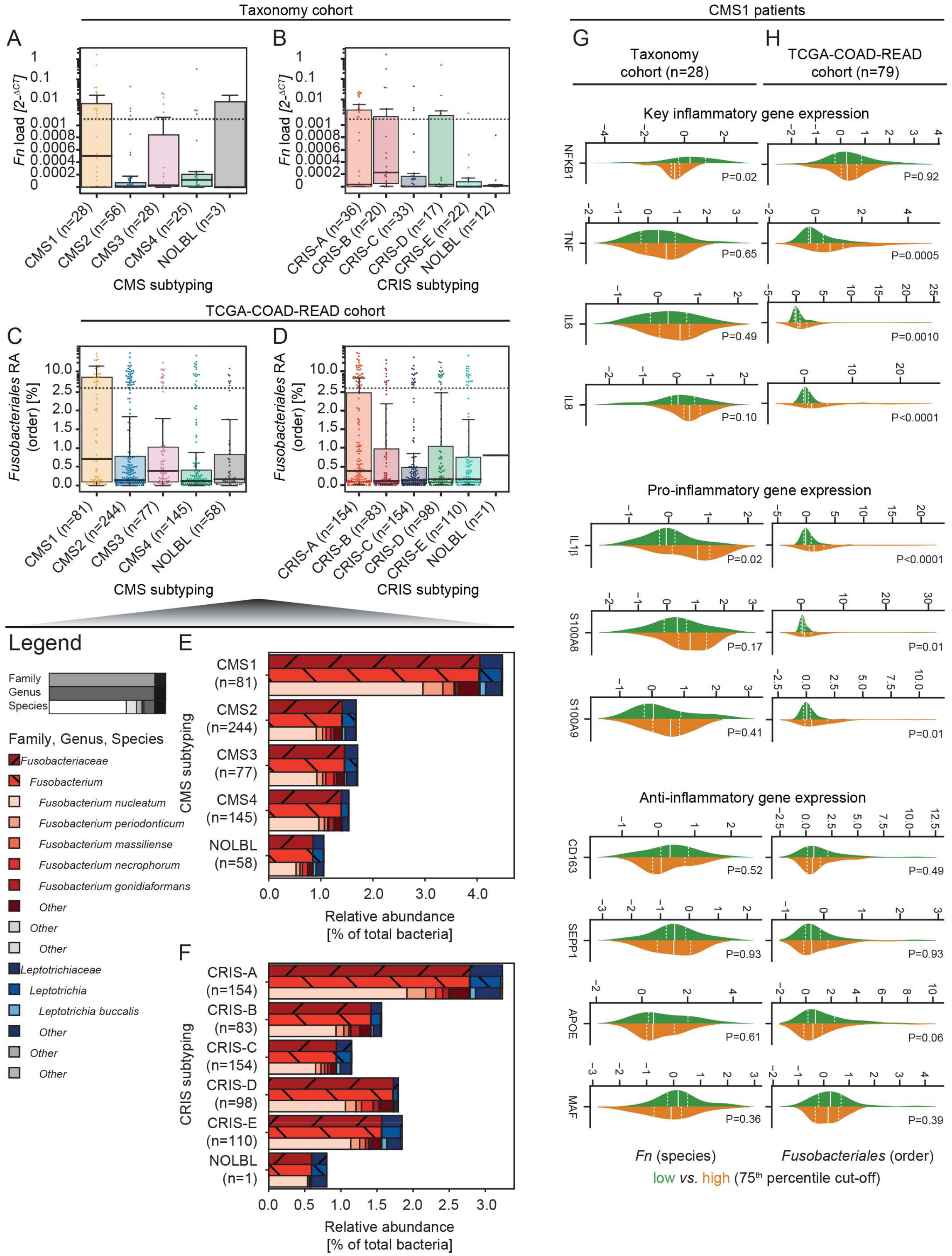

Figure 4 Prevalence of *Fn*/*Fusobacteriales* by transcriptomic-based molecular subtypes of the host. (A–D) Boxplot with overlaid dot plots displaying the dependency by CMS (A,C) and CRIS (B,D) molecular subtyping by either *Fn* load (Taxonomy cohort; A,B) or *Fusobacteriales* RA at the order taxonomic rank (TCGA-COAD-READ cohort; C,D). (E,F) RA (to total bacterial kingdom) of *Fusobacteriales* reported at increasing resolution of taxonomic rank (family, genus and species) by CMS (E) and CRIS (F) subtypes (aggregated by mean). Genuses/species with an average RA lower than 0.05 were aggregated as 'other'. (G,H) Distribution of key (pro-)/(anti-)inflammatory genes in CMS1 patients classified as -low (in green) or -high (in orange) using the 75th percentile as cut-off. Patients' stratification was based on either *Fn* load (Taxonomy cohort (G) or *Fusobacteriales* RA at the order taxonomic rank (TCGA-COAD-READ cohort, H). Median and lower (25th) and upper (75th) percentiles are indicated by white solid or dashed lines, respectively. (Unadjusted) P values were determined by Kruskal-Wallis tests. CMS, consensus molecular subtyping; CRIS, colorectal cancer intrinsic subtyping; *Fn*, *Fusobacterium nucleatum*; RA, relative abundance; TCGA-COAD-READ, colon and rectal cases of The Cancer Genome Atlas.

Fn/*Fusobacteriales* may play an active role in mediating inflammation in the host.

Patients with high *Fn*/*Fusobacteriales* have worse outcome in CMS4/CRIS-B

We sought to investigate whether bacterium presence correlated with patient clinical outcome assessed by overall survival (OS), disease-specific survival (DSS) and disease-free survival (DFS) endpoints (figure 5 and online supplemental figures 9 and 10).

We found no statistically significant differences in either cohort when comparing survival curves from patients grouped by either *Fn* load or *Fusobacteriales* RA (figure 5A,E,I and online supplemental figure 9-10). We hypothesised that *Fn*/*Fusobacteriales* may result in poorer outcome in a subtype-dependent context (ie, mesenchymal status; figure 5B,F,J). Indeed, we identified a differential association between *Fusobacteriales* RA and clinical outcome of the TCGA-COAD-READ cohort in mesenchymal (either CMS4 and/or CRIS-B) versus non-mesenchymal (neither CMS4 nor CRIS-B) tumours (figure 5G,H,K,L and online supplemental figure 10). *Fusobacteriales*-high mesenchymal patients had approximately twofold higher risk of worse outcome, whereas these associations were null in non-mesenchymal patients (figure 5G,H,K,L and online supplemental figure 10). Importantly, these findings held true when accounting for key (adjusted model 1) and more extensive (adjusted model 2) clinical–pathological characteristics that may represent confounders or disease modifiers (online supplemental table 7). We fitted two additional Cox regression models where, in addition to the interaction term between *Fusobacteriales* and mesenchymal status, we included adjustment covariates. In adjusted model 1, we included age, stage, tumour location and sex as key clinicopathological and demographic covariates. In adjusted model 2, we expanded on adjusted model 1 by also including history of colon polyps and history of other malignancy as comorbidities. We found that the risk of unfavourable outcome (HRs) and statistical significance were minimally impacted by accounting for potential disease modifiers in adjusted models 1 and 2, confirming the robustness of our findings (online supplemental table 7).

Although numbers in the Taxonomy cohort are more limited, when restricting the analysis to CMS4 and/or CRIS-B cases, we observed a trend in which *Fn*-high patients had shorter OS than those with low *Fn* load. Again, no difference in survival according to *Fn* load was observed in non-mesenchymal Taxonomy patients (figure 5C and online supplemental figure 9).

Exploratory analyses examining the association between clinical outcome and pathogen prevalence at taxonomic ranks of increasing resolution (order, family, genus and species) in the TCGA-COAD-READ cohort by fitting Cox regression models on the whole unselected population and in mesenchymal versus non-mesenchymal settings revealed that the prognostic impact stems primarily from, but is not limited to, species, including *Fn*, from the *Fusobacterium* genus from the *Fusobacteriaceae* family (figure 5M and online supplemental figure 11).

Putative mechanisms underlying selective *Fusobacteriales* virulence in mesenchymal tumours

Having identified a patient subpopulation that has an unfavourable clinical outcome when their tumours exhibit mesenchymal traits and are highly positive with *Fn*/*Fusobacteriales*, we reasoned that intervening by either clearing *Fn*/*Fusobacteriales* with broad-spectrum antibiotics or targeting the host–tumour biology could ameliorate clinical outcome for this subpopulation of patients. Given that broad-spectrum antibiotics may not represent a viable avenue in the clinic and narrow-spectrum antibiotics currently do not exist, we set out to identify clinically actionable host-specific vulnerabilities that could be exploited. We examined the host signalling pathways and microenvironment to identify alterations that may be mediated by and/or exacerbated by *Fusobacteriales* (ie, interact) and, thus, may promote virulence and, ultimately, result in an unfavourable clinical outcome. To disentangle the three-way association between *Fusobacteriales* RA, gene/signature and molecular subtyping, we fitted two distinct logistic regression models for each feature of interest in the TCGA-COAD-READ cohort. The selection of features was hypothesis-driven and included key host signalling pathways and immunomodulators (figure 6A).

Figure 6A reports p values from the two models capturing the association between *Fusobacteriales* RA (high vs low) and either each gene/signature (model 1: *Fusobacteriales*~*gene/signature*, x-axis) or the interaction between each gene/signature with the molecular subtype (model 2: *Fusobacteriales*~*gene/signature*×*molecular subtype*, y-axis). The top half quadrant (darker grey shaded area) identifies a set of genes/signatures whose expression patterns differ by molecular subtype (statistically significant interaction p value in model 2) and thus may be mediating the signalling impact of *Fusobacteriales* and were prioritised for downstream analyses (figure 6B).

We tested whether the gene/signature we identified as candidate targets are indeed related to clinical outcome in patients of the TCGA-COAD-READ cohort with mesenchymal tumours and high *Fusobacteriales*. We restricted our analysis to patients with mesenchymal tumours, and for each clinical endpoint of interest, namely, OS, DSS or DFS, we fitted Cox regression models with an interaction term for *Fusobacteriales* RA (low vs high) and each of the gene/signature (low vs high) identified as statistically significant in the analysis presented in figure 6A. We reasoned that a gene/signature could be considered a candidate target with both specific and translatable impact on clinical outcome for patients with mesenchymal tumours if its association with unfavourable clinical outcome differed by *Fusobacteriales*. This analysis identified CSF1-3, IL-1β, IFN-γ, IL-8, IL-6, CD163, NOTCH2, ZEB2 and TFF2 as potential targets for patients with mesenchymal tumours and high *Fusobacteriales* (figure 6C and online supplemental figures 12–14).

DISCUSSION

Fusobacteriales, predominantly *Fn*, have been associated[5 6 8 11 20–26] with pathogenesis, progression and treatment response in CRC. We coupled mechanistic studies in cell cultures with hypothesis-driven and unbiased screening in clinically relevant and *omics*-rich CRC cohorts to examine the cross-talk between pathogen–host and pathogen–tumour microenvironment. We demonstrate relationships between *Fn*/*Fusobacteriales* prevalence and host immunity, signalling and transcriptomic-based molecular subtypes. Our findings suggest that host–pathogen interactions can define patient subpopulations where *Fn*/*Fusobacteriales* play an active or opportunistic role, depending on the underlying host–tumour biology and microenvironment and identify putative druggable and clinically actionable vulnerabilities.

We observed higher *Fn*/*Fusobacteriales* prevalence in CMS1 patients, corroborating findings by Purcell *et al*.[27] Interestingly, we found that overall, higher pathogen prevalence did not correlate with poorer disease outcome. In contrast, high *Fn*/*Fusobacteriales* levels were associated with poor prognosis in the CMS4/CRIS-B patient subset, suggesting that the presence of *Fn*/*Fusobacteriales*

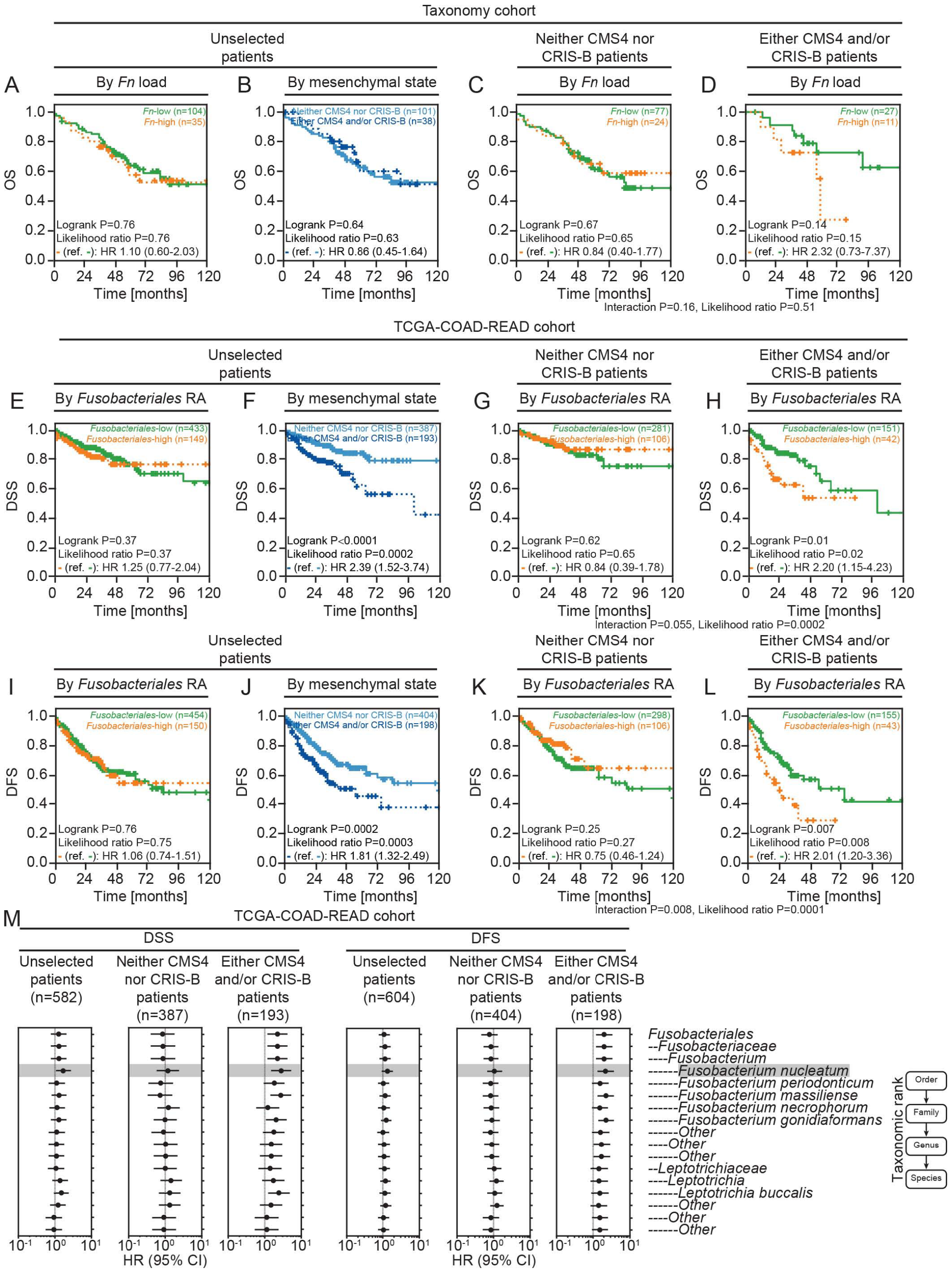

Figure 5 High *Fn*/*Fusobacteriales* prevalence is associated with negative clinical outcome in patients with mesenchymal-like tumours. (A–L) Kaplan-Meier estimates comparing survival curves in patients of the Taxonomy (OS, A–D) and TCGA-COAD-READ (DSS and DFS cohorts, E–L). Patients across the whole cohort were grouped by bacterium subgroup (low, in green, vs high, in orange; A,E,I) or mesenchymal status (CMS4 and/or CRIS-B, in light blue, vs remaining cases, in dark blue; B,F,J). Patients were grouped by bacterium group and further stratified by mesenchymal status (C,D,G,H,K,L). Patients were binned into a bacterium group (low vs high) using the 75th percentile as cut-off and based on either *Fn* load (Taxonomy cohort; A,C–D) or *Fusobacteriales* RA at the order level (TCGA-COAD-READ cohort; E,G–I,K,L). (M) Cox regression models fitted on bacterium RA reported at the order, family, genus and species taxonomic ranks. for each taxonomic rank, patients were classified as low or high subgroup using the corresponding 75th percentile RA abundance as cut-off. Univariate Cox regression models were fitted when evaluating the association between bacterium subgroup (high vs low, reference low) at each taxonomic rank and either DSS or DFS in the whole unselected patient population (left panel). Cox regression models with an interaction term between bacterium subgroup (high vs low; reference low) and mesenchymal status (mesenchymal, ie, either CMS4 and/or CRIS-B, vs non-mesenchymal, ie, neither CMS4 nor CRIS-B) at each taxonomic rank and either DSS or DFS was fitted to evaluate differential impact of bacterium on clinical outcome by tumour biology (right panels). CMS, consensus molecular subtyping; CRIS, colorectal cancer intrinsic subtyping; DFS, disease-free survival; DSS, disease-specific survival; *Fn*, *Fusobacterium nucleatum*; OS, overall survival; TCGA-COAD-READ, colon and rectal cases of The Cancer Genome Atlas.

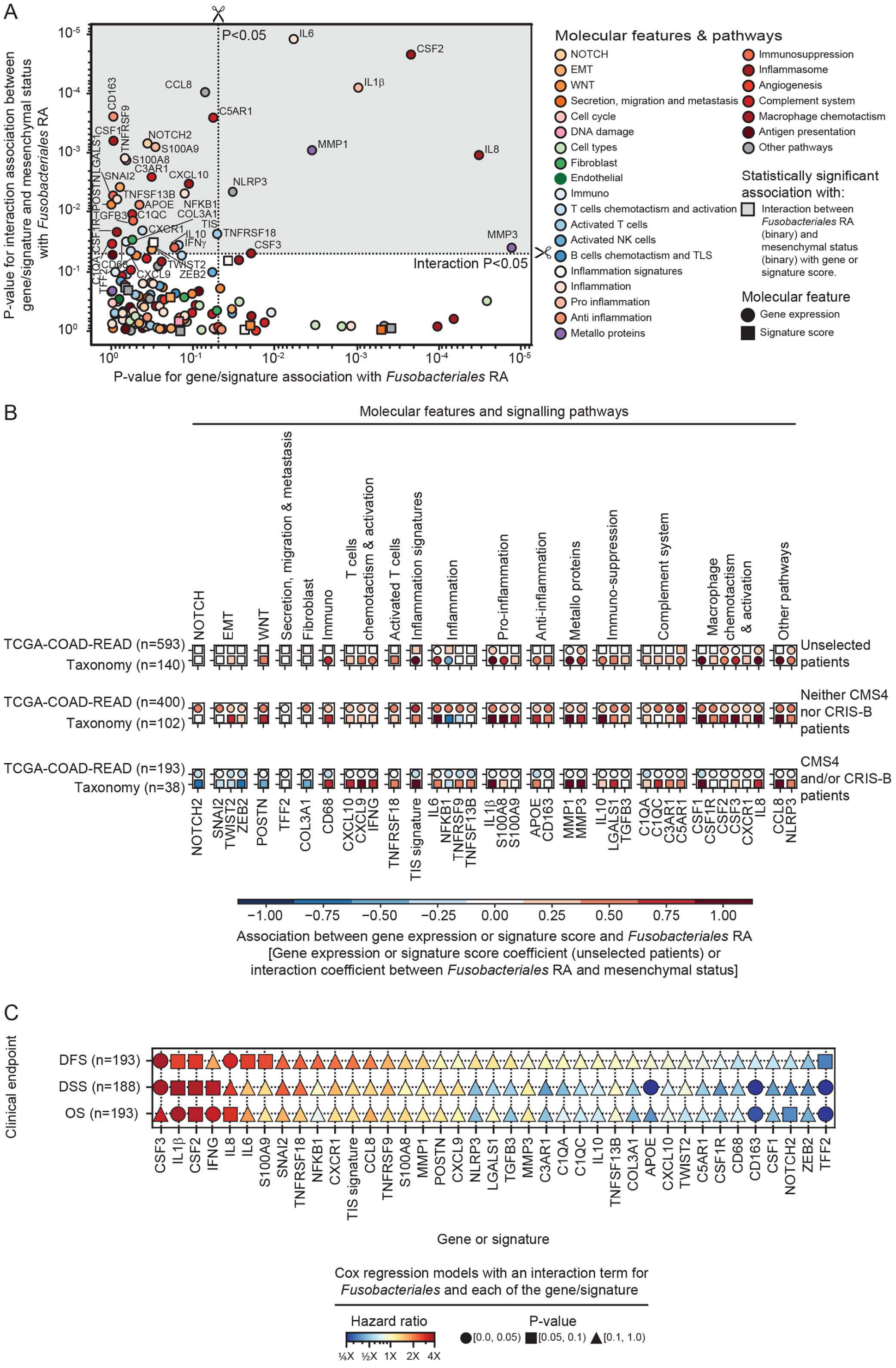

Figure 6 Exploration of mechanism underlying differential impact of *Fn*/*Fusobacteriales* in mesenchymal versus non-mesenchymal tumours. (A) Scatterplot depicting p values derived by assessing with logistic regression models the relationship between genes/signatures associated with *Fusobacteriales* RA in univariate analysis (model 1, x-axis) or the interaction with mesenchymal status (model 2, y-axis). Gene/signature with statistically significant p values from model 2 are highlighted by a grey shaded area. (B) Breakdown of association including direction and effect size, in the unselected patients' population and within mesenchymal versus non-mesenchymal cases. Only gene/signatures with significant interaction between *Fusobacteriales* RA and the gene/signature interaction with the molecular subtype (model 2, top quadrant, grey-shaded area) in the TCGA-COAD-READ cohort are included. Associations for both the TCGA-COAD-READ (*Fusobacteriales* RA) and Taxonomy (*Fn* load) cohorts are shown. Statistically significant associations are represented with circle markers, whereas non-significant associations are indicated by squared markers. (C) Association between gene/signature identified as candidate targets, A) and clinical outcome in patients of the TCGA-COAD-READ cohort with mesenchymal tumours. HRs and p values are derived from Cox regression models with an interaction term for *Fusobacteriales* relative abundance (low vs high) and each of the gene/signature (low vs high) being evaluated. CMS, consensus molecular subtyping; CRIS, colorectal cancer intrinsic subtyping; DFS, disease-free survival; DSS, disease-specific survival; *Fn*, *Fusobacterium nucleatum*; OS, overall survival; TCGA-COAD-READ, colon and rectal cases of The Cancer Genome Atlas.

has a specific clinical impact in mesenchymal-rich, high-stromal infiltrated tumours; this argues against a blanket approach for treating patients with *Fn*/*Fusobacteriales*-high tumours. Treatment with wide spectrum antibiotics reduces the growth of *Fn*-positive tumours in vivo.[8] However, the use of antibiotics to treat *Fn*-positive CRC tumours may be limited as *Fn* penetrate deeply within tumour, immune and endothelial cells where they internalise with endosomes and lysosomes,[28] adapt[29] and persist.[8] In addition, long-term use of antibiotics can cause gut dysbiosis, which may impact disease progression and outcome.

Given that 'it takes two to tango', namely, a high pathogen prevalence and a conducive host milieu, we further examined this interdependence to identify druggable aberrations in the host signalling pathways and microenvironment. We identified putative targets related to (pro-)inflammation, inflammasome, activated T cells, complement system, metalloproteins and macrophage chemotaxis and activation. *Fusobacteriales* induce a constitutively activated NFκB-TNF-α-IL-6 state which results in activation of metalloproteins and inflammatory cytokines (CSF1-3) which mediate macrophage differentiation, inhibit cytotoxic immune cells and promote proliferation of myeloid-derived-suppressor (MDSC) cells. We observed an increase in inflammation and M1 macrophages and a decrease in M2 macrophages in patients with higher *Fn*/*Fusobacteriales* prevalence. We envisage that therapeutic options, such as NLRP3/AIM2 inflammasome suppression,[30] IL-1β blockade,[31] TNF-α[32] or IL-6 inhibition,[33] which have been approved for treatment of chronic inflammation and cytokine storm syndrome in multiple cancers, rheumatoid arthritis and COVID-19 may ameliorate the immunosuppressive microenvironment induced by *Fn*/*Fusobacteriales*. Importantly, these targets are involved in not only promoting an immunosuppressive microenvironment by recruiting tissue-associated macrophages (TAMs) and MDSCs, but also in orchestrating invasion, angiogenesis, epithelial-to-mesenchymal transition and, ultimately, metastasis. The prometastatic impact of *Fn*/*Fusobacteriales* is further corroborated by findings in the literature linking higher pathogen prevalence in more advanced disease stage and metastasis in clinical specimens[5] and higher metastatic burden in mice inoculated with *Fn*.[34]

Cancer cells with an EMT phenotype secrete cytokines such as IL-10 and TGF-β that can further promote an immunosuppressive microenvironment. Additionally, secretion of IL-6 and IL-8 from stroma cells can further foster an EMT phenotype, activate primary fibroblasts (cancer-associated fibroblast (CAFs)) which, in turn, may promote angiogenesis and invasion.[35] Taken together, these aberrations may result in a self-reinforcing mechanism that confers on cancer cells the ability to migrate, invade the extracellular matrix, extravasate and seed metastasis. When comparing the transcriptomic profiles by *Fusobacteriales* RA in the TCGA-COAD-READ cohort, we identified dysregulation affecting cell architecture involving apical surface dynamics and Aurora A kinase signalling, which regulate cMYC, DNA repair, cell motility/migration and induce EMT transition via β-catenin and TGF-β, leading to metastasis and resistance to treatment in multiple cancer types.[36] Small molecule inhibitors against Aurora A have shown encouraging results in preclinical studies and clinical trials in CRC[37] and other cancers.[38] Cytoskeleton shape, filopodium protrusions and alterations in cell adhesion and structure are hallmarks of extracellular matrix invasion. EMT key effectors, SNAIL and ZEB1, alter apical surface dynamics by inhibiting scaffolding proteins and by inducing expression of matrix metalloproteins (MMP3 and MMP9), resulting in loosened tight junctions, altered cell polarity and increased plasticity which, in turn, enable cell invasion.[39] Dysregulations in MMP expression may aid cancer cells that have reached the bloodstream to extravasate to distant tissues[40] by priming the vascular endothelium via upregulation of VEGF-A[41] and by increasing permeability via COX2 upregulation.[42] Our analyses in the TCGA-COAD-READ cohort identified higher expression of vascular endothelial growth factor (VEGF) as well as an angiogenesis signature in patients with higher *Fusobacteriales* RA. Indeed, a new generation of selective and highly penetrative MMP inhibitors[43] is being trialled in GI cancers,[44] and Mehta *et al* reported lower *Fusobacteriales* RA in subjects treated with aspirin, a COX2 inhibitor.[45]

Green *et al*[46] demonstrated that MAPK7 is a master regulator of MMP9 and promotes the formation of metastasis. We observed a dysregulation in MAPK signalling at the protein level when comparing *Fusobacteriales*-high versus *Fusobacteriales*-low patients of the TCGA-COAD-READ cohort. MAPK7 induces EMT transition, cell migration and regulates TAM polarisation in a metalloprotein-dependent manner,[46] rendering it an appealing upstream therapeutic target. IL-6 orchestrates MAPK-STAT3 signalling, which in turn regulates the dynamic transition between two CAFs subpopulations, EMT-CAFs and proliferation-CAFs,[47] rendering the IL-6-TGF-β-EMT-CAFs cross-talk potentially a further therapeutic target. While directly targeting EMT via NOTCH or WNT has shown limited success in the clinic,[48] microenvironment remodelling to reverse immunosuppression by inhibiting CXCL12[49] or promoting T-cell infiltration[50] or function via engineered oncolytic adenovirus,[51] has shown promising results in reducing metastasis formation.[52] Additionally, we observed a positive correlation between gene expression of IL-8, CXCL8, CXCR1 and CXCL10 and *Fn*/*Fusobacteriales* prevalence, corroborating findings from Casasanta *et al.* assessing *Fn* in HCT116 CRC cells.[53]

In conclusion, our analyses have identified a patient subpopulation that has an unfavourable clinical outcome when their tumours exhibit mesenchymal traits and are highly positive with *Fn*/*Fusobacteriales* and pinpointed clinically actionable host-specific vulnerabilities that suggest new treatments for these patients that extend beyond broad-spectrum antibiotics.

Acknowledgements We thank the patients who kindly donated their samples and made this study possible.

Contributors MS, DL and JHMP conceptualised and designed the study. MS, NC, KS, SB, DL and JHMP were involved in collection, preparation, interpretation, validation and critical review of the data. NC and KS performed the cell culture experiments and quantified bacterium load in tumour samples of the patients of the Taxonomy cohort. MS performed formal analysis including bioinformatics and statistical analyses. MS created the manuscript figures and supplementary materials. MS and JHMP drafted the manuscript. All authors edited, reviewed, revised and approved the manuscript text. DL and JHMP acquired funding for the study.

Funding This study was supported by a grant from the Health Research Board and Science Foundation Ireland to JHMP (16/US/3301), a studentship to KS sponsored by The Northern Ireland Department for the Economy (NI DfE), and by funding from NI DfE (SFI-DEL 14/1A/2582, STL/5715/15). The results included here are in part based on data generated by the TCGA Research Network (https://wwwcancergov/tcga). We wish to acknowledge the information technology department at the Royal College of Surgeons in Ireland and the Irish Centre for High-End Computing (ICHEC) for the provision of computational facilities and support.

Competing interests None declared.

Patient consent for publication Not required.

Ethics approval The Taxonomy cohort collection was approved by the Medicine, Dentistry, and Biomedical Sciences School Ethics Committee (ref: 12/12v4), as previously described (Allen *et al*, JCO Precision Oncology, 2018; PMID: 30088816). Approval for the cohort of patients with colon (COAD) and rectal (READ) cases denotated as TCGA-COAD-READ in this manuscript was acquired by the original investigators of The Cancer Genome Atlas consortium.

Provenance and peer review Not commissioned; externally peer reviewed.

Data availability statement Data are available in a public, open access repository. Processing and analysis code along with bacterium estimates with corresponding clinical and molecular datasets for the Taxonomy and TCGA-COAD-READ cohorts included in this study are publicly available and archived at Zenodo (https://10.5281/zenodo.4019142). Bacterium estimates include *Fusobacterium nucleatum* load (Taxonomy cohort) and *Fusobacteriales* relative abundance, along with higher resolution estimates at genus, family and species taxonomic ranks, (TCGA-COAD-READ cohort).

Supplemental material This content has been supplied by the author(s). It has not been vetted by BMJ Publishing Group Limited (BMJ) and may not have been peer-reviewed. Any opinions or recommendations discussed are solely those of the author(s) and are not endorsed by BMJ. BMJ disclaims all liability and responsibility arising from any reliance placed on the content. Where the content includes any translated material, BMJ does not warrant the accuracy and reliability of the translations (including but not limited to local regulations, clinical guidelines, terminology, drug names and drug dosages), and is not responsible for any error and/or omissions arising from translation and adaptation or otherwise.

ORCID iD

Manuela Salvucci http://orcid.org/0000-0001-9941-4307

REFERENCES

1 Bray F, Ferlay J, Soerjomataram I, *et al*. Global cancer statistics 2018: GLOBOCAN estimates of incidence and mortality worldwide for 36 cancers in 185 countries. *CA Cancer J Clin* 2018;68:394–424.

2 Guinney J, Dienstmann R, Wang X, *et al*. The consensus molecular subtypes of colorectal cancer. *Nat Med* 2015;21:1350–6.

3 Isella C, Brundu F, Bellomo SE, *et al*. Selective analysis of cancer-cell intrinsic transcriptional traits defines novel clinically relevant subtypes of colorectal cancer. *Nat Commun* 2017;8:15107.

4 Routy B, Gopalakrishnan V, Daillère R, *et al*. The gut microbiota influences anticancer immunosurveillance and general health. *Nat Rev Clin Oncol* 2018;15:382–96.

5 Flanagan L, Schmid J, Ebert M, *et al*. Fusobacterium nucleatum associates with stages of colorectal neoplasia development, colorectal cancer and disease outcome. *Eur J Clin Microbiol Infect Dis* 2014;33:1381–90.

6 Brennan CA, Garrett WS. Fusobacterium nucleatum - symbiont, opportunist and oncobacterium. *Nat Rev Microbiol* 2019;17:156–66.

7 Ito M, Kanno S, Nosho K, *et al*. Association of Fusobacterium nucleatum with clinical and molecular features in colorectal serrated pathway. *Int J Cancer* 2015;137:1258–68.

8 Bullman S, Pedamallu CS, Sicinska E, *et al*. Analysis of *Fusobacterium* persistence and antibiotic response in colorectal cancer. *Science* 2017;358:1443–8.

9 Gethings-Behncke C, Coleman HG, Jordao HWT, *et al*. *Fusobacterium nucleatum* in the Colorectum and Its Association with Cancer Risk and Survival: A Systematic Review and Meta-analysis. *Cancer Epidemiol Biomarkers Prev* 2020;29:539–48.

10 Dharmani P, Strauss J, Ambrose C, *et al*. Fusobacterium nucleatum infection of colonic cells stimulates MUC2 mucin and tumor necrosis factor alpha. *Infect Immun* 2011;79:2597–607.

11 Kostic AD, Chun E, Robertson L, *et al*. Fusobacterium nucleatum potentiates intestinal tumorigenesis and modulates the tumor-immune microenvironment. *Cell Host Microbe* 2013;14:207–15.

12 Allen WL, Dunne PD, McDade S, *et al*. Transcriptional subtyping and CD8 immunohistochemistry identifies patients with stage II and III colorectal cancer with poor prognosis who benefit from adjuvant chemotherapy. *JCO Precis Oncol* 2018;21:1–15.

13 McCorry AM, Loughrey MB, Longley DB, *et al*. Epithelial-To-Mesenchymal transition signature assessment in colorectal cancer quantifies tumour stromal content rather than true transition. *J Pathol* 2018;246:422–6.

14 Kostic AD, Ojesina AI, Pedamallu CS, *et al*. PathSeq: software to identify or discover microbes by deep sequencing of human tissue. *Nat Biotechnol* 2011;29:393–6.

15 Walker MA, Pedamallu CS, Ojesina AI, *et al*. GATK PathSeq: a customizable computational tool for the discovery and identification of microbial sequences in libraries from eukaryotic hosts. *Bioinformatics* 2018;215:4287–9.

16 Finotello F, Mayer C, Plattner C, *et al*. Molecular and pharmacological modulators of the tumor immune contexture revealed by deconvolution of RNA-Seq data. *Genome Med* 2019;11:34.

17 Becht E, Giraldo NA, Lacroix L, *et al*. Estimating the population abundance of tissue-infiltrating immune and stromal cell populations using gene expression. *Genome Biol* 2016;17:218.

18 Mima K, Sukawa Y, Nishihara R, *et al*. *Fusobacterium nucleatum* and T Cells in Colorectal Carcinoma. *JAMA Oncol* 2015;1:653–61.

19 Mermel CH, Schumacher SE, Hill B, *et al*. GISTIC2.0 facilitates sensitive and confident localization of the targets of focal somatic copy-number alteration in human cancers. *Genome Biol* 2011;12:R41.

20 Castellarin M, Warren RL, Freeman JD, *et al*. Fusobacterium nucleatum infection is prevalent in human colorectal carcinoma. *Genome Res* 2012;22:299–306.

21 McCoy AN, Araújo-Pérez F, Azcárate-Peril A, *et al*. Fusobacterium is associated with colorectal adenomas. *PLoS One* 2013;8:e53653.

22 Kostic AD, Gevers D, Pedamallu CS, *et al*. Genomic analysis identifies association of Fusobacterium with colorectal carcinoma. *Genome Res* 2012;22:292–8.

23 Nosho K, Sukawa Y, Adachi Y, *et al*. Association of Fusobacterium nucleatum with immunity and molecular alterations in colorectal cancer. *World J Gastroenterol* 2016;22:557–66.

24 Kinross J, Mirnezami R, Alexander J, *et al*. A prospective analysis of mucosal microbiome-metabonome interactions in colorectal cancer using a combined MAS 1HNMR and metataxonomic strategy. *Sci Rep* 2017;7:8979.

25 Lee D-W, Han S-W, Kang J-K, *et al*. Association between Fusobacterium nucleatum, pathway mutation, and patient prognosis in colorectal cancer. *Ann Surg Oncol* 2018;25:3389–95.

26 Kunzmann AT, Proença MA, Jordao HW, *et al*. Fusobacterium nucleatum tumor DNA levels are associated with survival in colorectal cancer patients. *Eur J Clin Microbiol Infect Dis* 2019;38:1891–9.

27 Purcell RV, Visnovska M, Biggs PJ, *et al*. Distinct gut microbiome patterns associate with consensus molecular subtypes of colorectal cancer. *Sci Rep* 2017;7:11590.

28 Ji S, Shin JE, Kim YC, *et al*. Intracellular degradation of Fusobacterium nucleatum in human gingival epithelial cells. *Mol Cells* 2010;30:519–26.

29 Umaña A, Sanders BE, Yoo CC, *et al*. Utilizing Whole *Fusobacterium* Genomes To Identify, Correct, and Characterize Potential Virulence Protein Families. *J Bacteriol* 2019;201:e00273–19.

30 Hamarsheh Shaima'a, Zeiser R. Nlrp3 inflammasome activation in cancer: a double-edged sword. *Front Immunol* 2020;11.

31 Dinarello CA, Simon A, van der Meer JWM. Treating inflammation by blocking interleukin-1 in a broad spectrum of diseases. *Nat Rev Drug Discov* 2012;11:633–52.

32 Ortiz P, Bissada NF, Palomo L, *et al*. Periodontal therapy reduces the severity of active rheumatoid arthritis in patients treated with or without tumor necrosis factor inhibitors. *J Periodontol* 2009;80:535–40.

33 Choy EH, De Benedetti F, Takeuchi T, *et al*. Translating IL-6 biology into effective treatments. *Nat Rev Rheumatol* 2020;16:335–45.

34 Parhi L, Alon-Maimon T, Sol A, *et al*. Breast cancer colonization by Fusobacterium nucleatum accelerates tumor growth and metastatic progression. *Nat Commun* 2020;11:1–12.

35 Erez N, Truitt M, Olson P, *et al*. Cancer-Associated fibroblasts are activated in incipient neoplasia to orchestrate tumor-promoting inflammation in an NF-κB-dependent manner. *Cancer Cell* 2010;17:135–47.

36 Shah K, Ahmed M, Kazi JU. The Aurora kinase/β-catenin axis contributes to dexamethasone resistance in leukemia. *NPJ Precis Oncol* 2021;5:13.

37 Pitts TM, Bradshaw-Pierce EL, Bagby SM, *et al*. Antitumor activity of the Aurora a selective kinase inhibitor, alisertib, against preclinical models of colorectal cancer. *Oncotarget* 2016;7:50290–301.

38 Brockmann M, Poon E, Berry T, *et al*. Small molecule inhibitors of Aurora-A induce proteasomal degradation of N-myc in childhood neuroblastoma. *Cancer Cell* 2013;24:75–89.

39 Stemmler MP, Eccles RL, Brabletz S, *et al*. Non-Redundant functions of EMT transcription factors. *Nat Cell Biol* 2019;21:102–12.

40 Cox TR. The matrix in cancer. *Nat Rev Cancer* 2021;21:217–38.

41 Desch A, Strozyk EA, Bauer AT, *et al*. Highly invasive melanoma cells activate the vascular endothelium via an MMP-2/integrin αvβ5-induced secretion of VEGF-A. *Am J Pathol* 2012;181:693–705.

42 Lee KY, Kim Y-J, Yoo H, *et al*. Human brain endothelial cell-derived COX-2 facilitates extravasation of breast cancer cells across the blood-brain barrier. *Anticancer Res* 2011;31:4307–13.

43 Winer A, Adams S, Mignatti P. Matrix metalloproteinase inhibitors in cancer therapy: turning past failures into future successes. *Mol Cancer Ther* 2018;17:1147–55.

44 Bendell JC, Starodub A, Huang X, *et al*. A phase 3 randomized, double-blind, placebo-controlled study to evaluate the efficacy and safety of GS-5745 combined with mFOLFOX6 as first-line treatment in patients with advanced gastric or gastroesophageal junction adenocarcinoma. *JCO* 2017;35:TPS4139.

45 Mehta RS, Nishihara R, Cao Y, *et al*. Association of dietary patterns with risk of colorectal cancer subtypes classified by Fusobacterium nucleatum in tumor tissue. *JAMA Oncol* 2017;3:921.

46 Green D, Eyre H, Singh A, *et al*. Targeting the MAPK7/MMP9 axis for metastasis in primary bone cancer. *Oncogene* 2020;39:5553–69.

47 Ligorio M, Sil S, Malagon-Lopez J, *et al*. Stromal microenvironment shapes the intratumoral architecture of pancreatic cancer. *Cell* 2019;178:160–75.

48 Strosberg JR, Yeatman T, Weber J, *et al*. A phase II study of ro4929097 in metastatic colorectal cancer. *Eur J Cancer* 2012;48:997–1003.

49 Lang J, Zhao X, Qi Y, *et al*. Reshaping Prostate Tumor Microenvironment To Suppress Metastasis *via* Cancer-Associated Fibroblast Inactivation with Peptide-Assembly-Based Nanosystem. *ACS Nano* 2019;13:12357–71.

50 Tauriello DVF, Palomo-Ponce S, Stork D, *et al*. Tgfβ drives immune evasion in genetically reconstituted colon cancer metastasis. *Nature* 2018;554:538–43.

51 Freedman JD, Duffy MR, Lei-Rossmann J, *et al*. An oncolytic virus expressing a T-cell Engager simultaneously targets cancer and immunosuppressive stromal cells. *Cancer Res* 2018;78:6852–65.

52 Ping Q, Yan R, Cheng X, *et al*. Correction: cancer-associated fibroblasts: overview, progress, challenges, and directions. *Cancer Gene Ther* 2021. doi:10.1038/s41417-021-00343-3. [Epub ahead of print: 28 Jun 2021].

53 Casasanta MA, Yoo CC, Udayasuryan B, *et al*. *Fusobacterium nucleatum* host-cell binding and invasion induces IL-8 and CXCL1 secretion that drives colorectal cancer cell migration. *Sci Signal* 2020;13:eaba9157.

Supplementary Figures for

"Patients with mesenchymal tumours and high *Fusobacteriales* prevalence have worse prognosis in colorectal cancer (CRC)"

Manuela Salvucci[1], Nyree Crawford[2], Katie Stott[2], Susan Bullman[3,4], Daniel B. Longley[2], and Jochen H.M. Prehn[1]*

[1]Centre for Systems Medicine, Department of Physiology and Medical Physics, Royal College of Surgeons in Ireland, Dublin, Ireland;

[2]Patrick G. Johnston Centre for Cancer Research, School of Medicine, Dentistry and Biomedical Science, Queen's University Belfast, Northern Ireland, UK;

[3]Dana-Farber Cancer Institute, Harvard Medical School, Boston, USA;

[4]Fred Hutchinson Cancer Research Center, Human Biology Division, Seattle, USA.

Corresponding author: Prof. Jochen H. M. Prehn, Department of Physiology and Medical Physics, Royal College of Surgeons in Ireland, 123 St. Stephen's Green, Dublin 2, Ireland. Tel.: +353-1-402-2255; Fax: +353-1-402-2447; E-mail: jprehn@rcsi.ie.

Data and code availability: Datasets and source code will be publicly available and archived upon publication at Zenodo (https://10.5281/zenodo.4019142).

Transcriptomic-dependent *Fn/Fusobacteriales* impact.

Supplementary Figure 1.

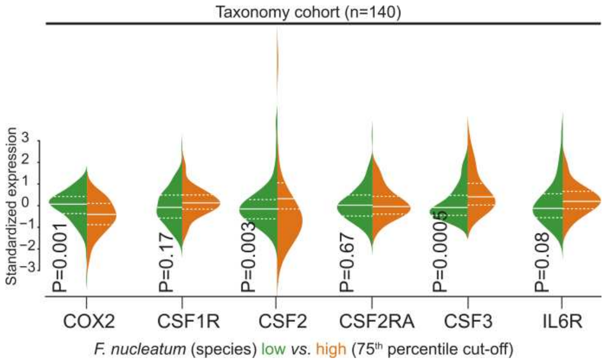

Association between Fn load and inflammation signalling in the human host.

Distribution of key player genes grouped by *Fn* (high vs. low, using the 75th percentile as cut-off) for patients of the Taxonomy cohort.

Median and lower (25th) and upper (75th) percentiles are indicated by white solid or dashed lines, respectively. Statistical significance was evaluated Kruskal-Wallis tests and P-values are reported.

Salvucci et al.

Supplementary Figure 2.

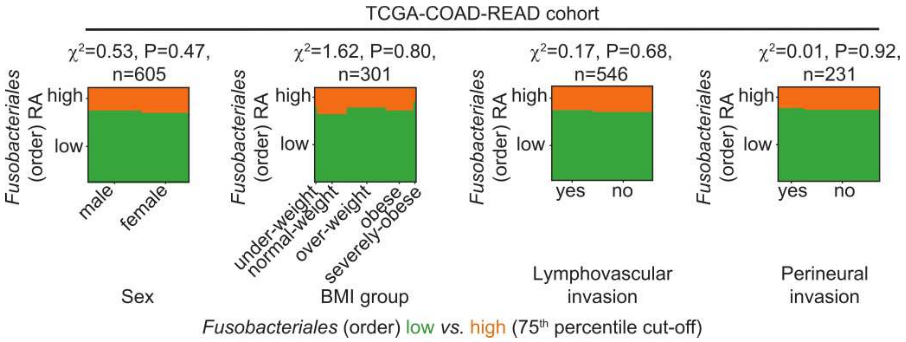

Association between Fusobacteriales relative abundance (RA) and human host clinico-pathological features in the TCGA-COAD-READ cohort.

Mosaic plots depicting the relationship between categorical clinico-pathological characteristics of the human host and *Fusobacteriales* RA. Patients were classified as *Fusobacteriales*-low or -high using the 75th percentile as cut-off and indicated in green and orange, respectively. Statistical significance was evaluated with χ^2 independence tests and the χ^2 test statistic and the mod-log-likelihood P-values are reported.

Abbreviations. BMI: body mass index.

Transcriptomic-dependent *Fn/Fusobacteriales* impact.

Supplementary Figure 3.

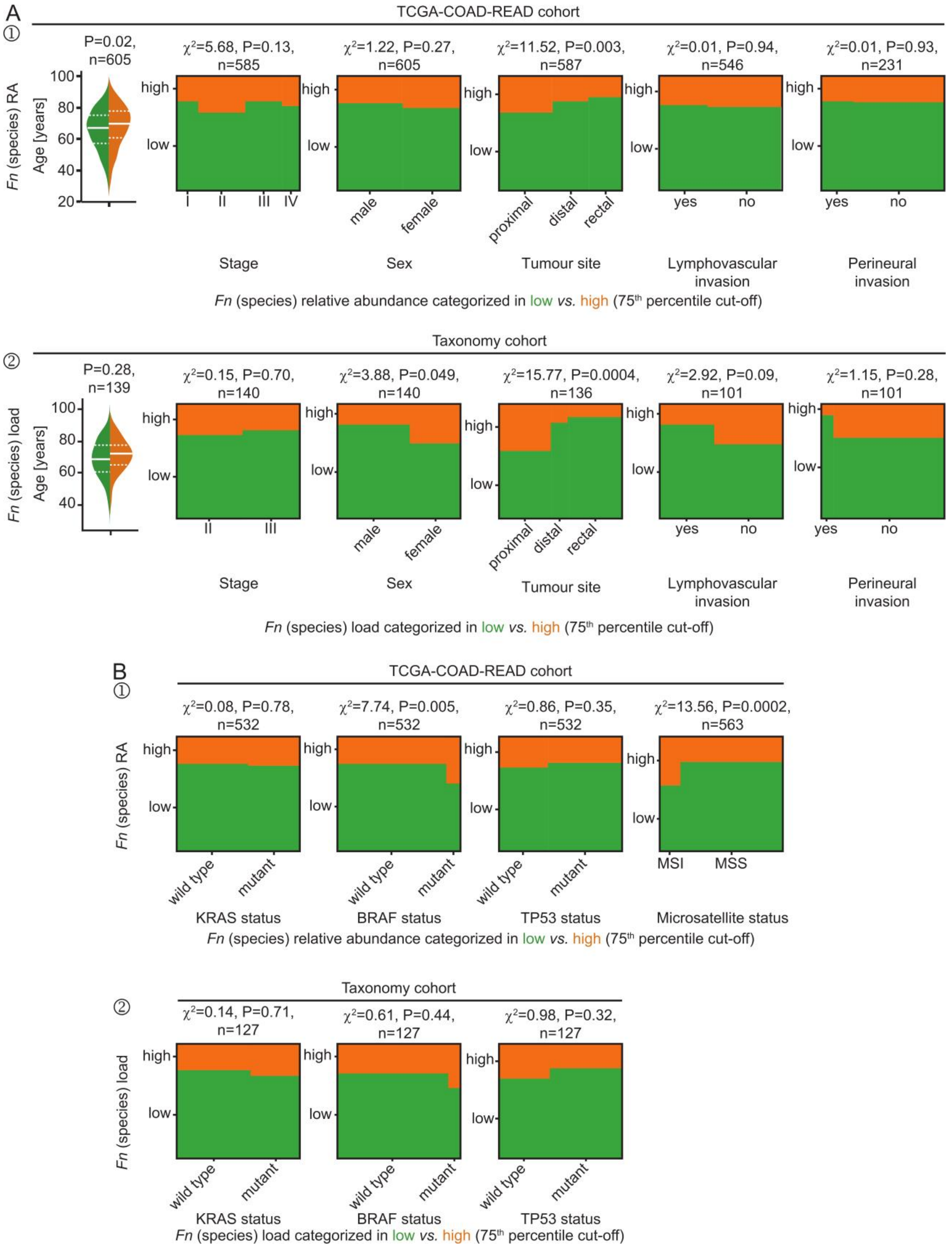

Salvucci et al.

Association between human host clinico-pathological (A) and mutational (B) features in Fn-low vs. high patients of the TCGA-COAD-READ (1) and Taxonomy (2) cohorts.

Fn is expressed as relative abundance (RA) for patients of the TCGA-COAD-READ cohort or load for patients of the in-house Taxonomy cohort. Patients were categorised in low vs. high subgroups using the 75th percentile as cut-off and indicated in green and orange, respectively. Association between *Fn* and continuous variables is depicted with violin plots, median and lower (25th) and upper (75th) percentiles are indicated by white solid or dashed lines, respectively. Statistical significance was evaluated Kruskal-Wallis tests and P-values are reported. Association between *Fn* and categorical clinico-pathological characteristics is depicted with mosaic plots and statistical significance was evaluated with χ^2 independence tests and the χ^2 test statistic and the mod-loglikelihood P-values are reported.

Supplementary Figure 4.

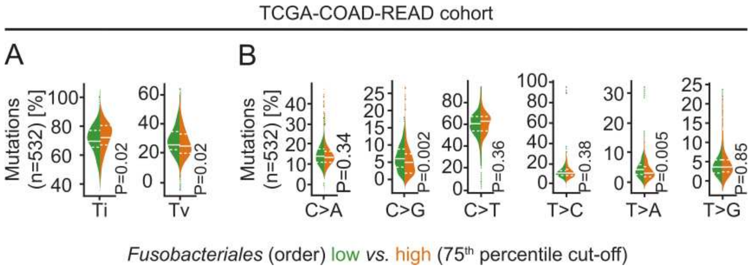

Association between Fusobacteriales relative abundance (RA) and DNA substitution mutations in the patients of TCGA-COAD-READ cohort.

A-B. Distribution of transitions (Ti) and transversions (Tv) (**A**) and conversion changes (**B**) in patients of the TCGA-COAD-READ cohort classified as *Fusobacteriales*-low (in green) or -high (in orange) based on a 75th percentile cut-off. Median and lower (25th) and upper (75th) percentiles are indicated by white solid or dashed lines, respectively. Statistical significance was evaluated Kruskal-Wallis tests and P-values are reported.

Transcriptomic-dependent *Fn/Fusobacteriales* impact.

Supplementary Figure 5.

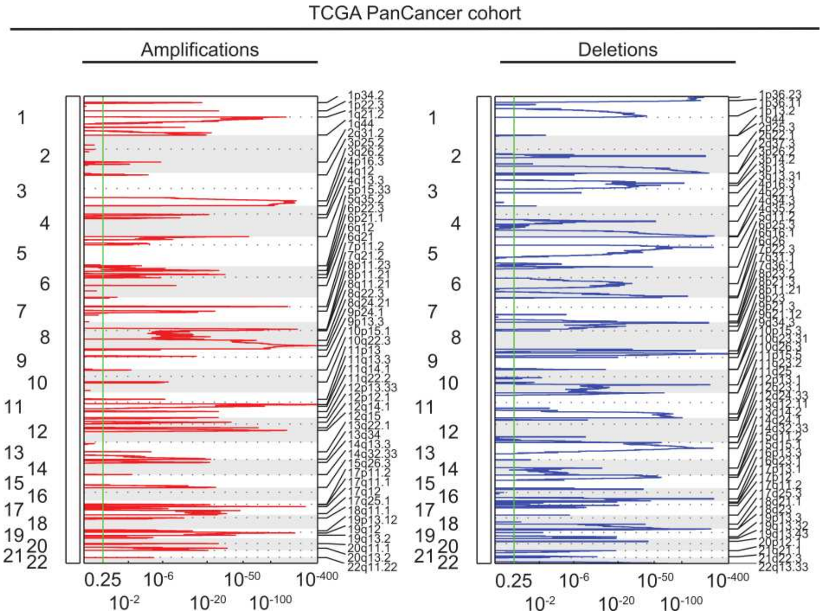

Recurrent copy number alterations in patients of the TCGA PanCancer cohort.

Amplifications (in red, left hand-side) and deletions (in blue, right hand-side) computed by GISTIC2 analysis to detect recurrent copy number alterations in the TCGA PanCancer cohort (n=9142).

Chromosome bands are indicated (y axis) and cytobands that reached statistical significance (as indicated by q-values) are shown.

Supplementary Figure 6.

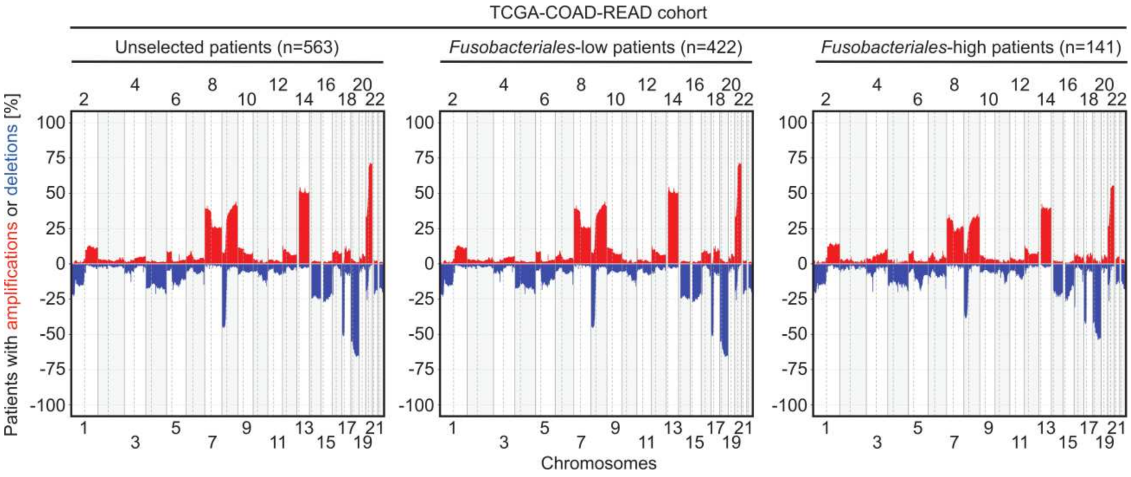

Frequency of copy number alterations in patients of the TCGA-COAD-READ cohort.

Frequency of occurrence of copy number amplifications (in red) or deletions (in blue) by chromosome in the whole unselected cohort (left panel) and in subgroups restricted to cases with low- (middle panel) or high- (right panel) *Fusobacteriales* relative abundance for patients of the TCGA-COAD-READ cohort.

Supplementary Figure 7.

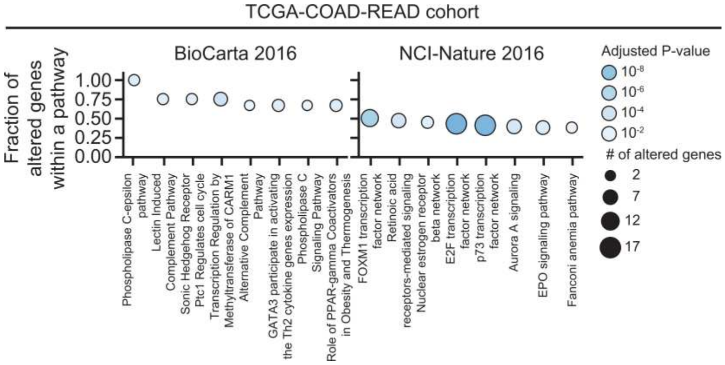

Pathway enrichment analysis for genes differentially expressed by Fusobacteriales relative abundance (RA) in patients of the TCGA-COAD-READ cohort.

Enrichment analysis on genes identified as differentially expressed by *Fusobacteriales* RA in patients of the TCGA-COAD READ cohort. Analysis was performed with *EnrichR* querying the *BioCarta* (version 2016) and *NCI-Nature* (version 2016) pathway databases. The number of identified altered genes for each pathway is encoded by the marker size and the magnitude of the associated P-values is color-coded, as indicated in the legend.

Supplementary Figure 8.

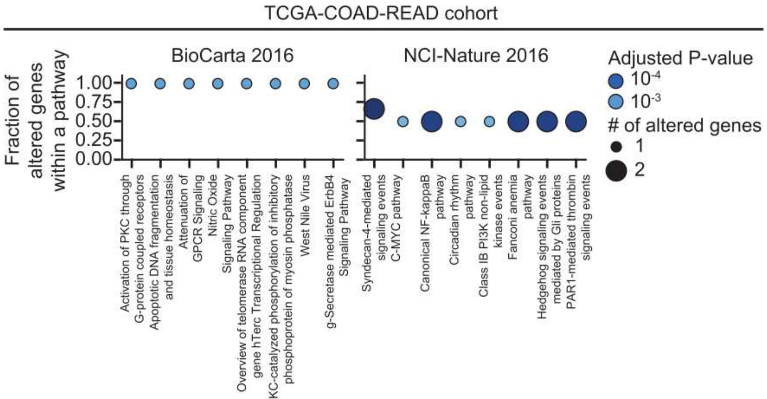

***Pathway enrichment analysis for proteins differentially expressed by Fusobacteriales relative abundance (RA) in patients of the TCGA-COAD-READ cohort*.**

Enrichment analysis on proteins identified as differentially expressed by *Fusobacteriales* RA in patients of the TCGA-COAD READ cohort. Analysis was performed with *EnrichR* querying the *BioCarta* (version 2016) and *NCI-Nature* (version 2016) pathway databases. The number of identified altered genes for each pathway is encoded by the marker size and the magnitude of the associated P-values is color-coded, as indicated in the legend.

Supplementary Figure 9.

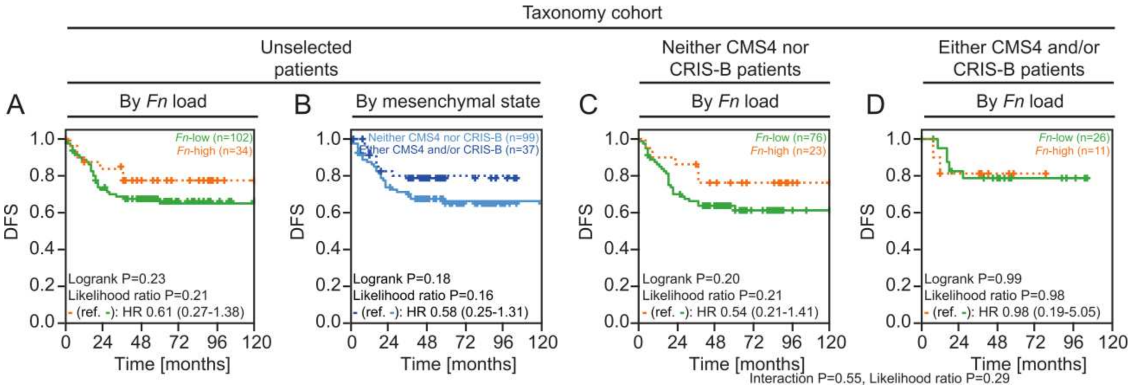

Kaplan-Meier plots comparing disease-free-survival (DFS) in patients of the Taxonomy cohort grouped by *Fn* load (**A**), mesenchymal status (**B**) and by *Fn* load within the non-mesenchymal and mesenchymal patients' subpopulations (**C-D**). Patients were categorised in *Fn*-low or -high subgroups using the 75th percentile as cut-off. *Consensus Molecular Subtype* (CMS) and *Cancer Intrinsic Subtype* (CRIS) assignments were used to categorise patients in non-mesenchymal ("Neither CMS4 nor CRIS-B") or mesenchymal, respectively ("Either CMS4 and/or CRIS-B").

Transcriptomic-dependent *Fn/Fusobacteriales* impact.

Supplementary Figure 10.

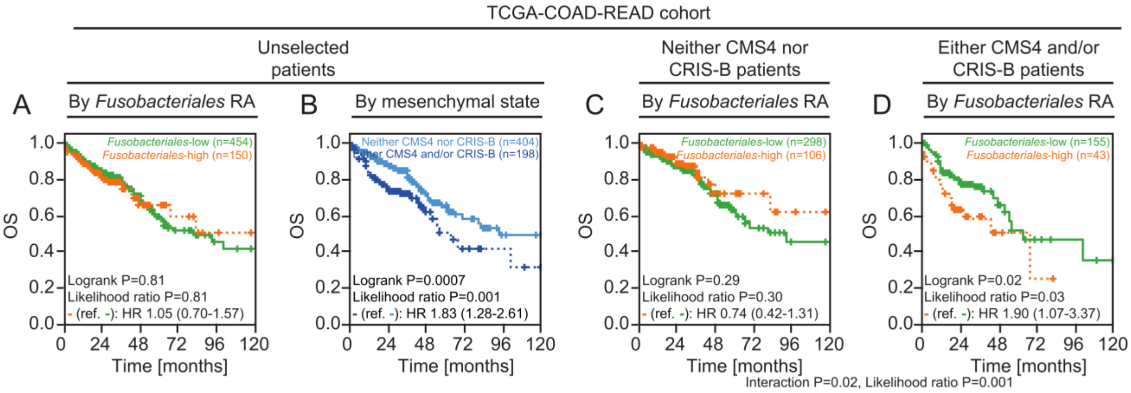

Kaplan-Meier plots comparing overall survival (OS) in patients of the TCGA-COAD-READ cohort grouped by *Fusobacteriales* RA (**A**), mesenchymal status (**B**) and by *Fusobacteriales* RA within the non-mesenchymal and mesenchymal patients' subpopulations (**C-D**). Patients were categorised in *Fusobacteriales*-low or -high subgroups using the 75th percentile as cut-off. *Consensus Molecular Subtype* (CMS) and *Cancer Intrinsic Subtype* (CRIS) assignments were used to categorise patients in non-mesenchymal ("Neither CMS4 nor CRIS-B") or mesenchymal, respectively ("Either CMS4 and/or CRIS-B").

Transcriptomic-dependent *Fn/Fusobacteriales* impact.

Supplementary Figure 11.

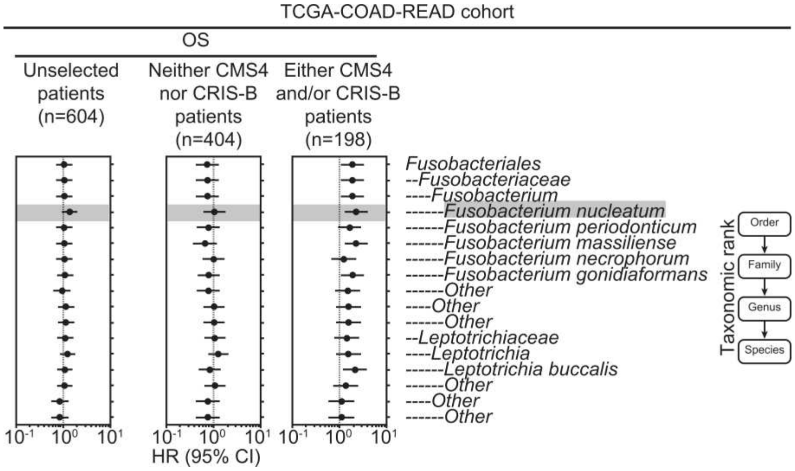

Cox regression models fitted on bacterium relative abundance reported at the order, family, genus, and species taxonomic ranks. For each taxonomic rank, patients were binned into -low or -high subgroups using the corresponding 75th percentile RA as cut-off. Univariate Cox regression models were fitted when evaluating association between bacterium subgroup (high vs. low; reference low) at each taxonomic rank and OS in the whole unselected patient population (left panel). Cox regression models with an interaction term between bacterium subgroup (high vs. low; reference low) and mesenchymal status (mesenchymal, i.e either CMS4 and/or CRIS-B, vs. non-mesenchymal, i. e. neither CMS4 nor CRIS-B) at each taxonomic rank and OS were fitted to evaluate differential impact of bacterium on clinical outcome by tumour biology (right panels).

Salvucci et al.

Supplementary Figure 12.

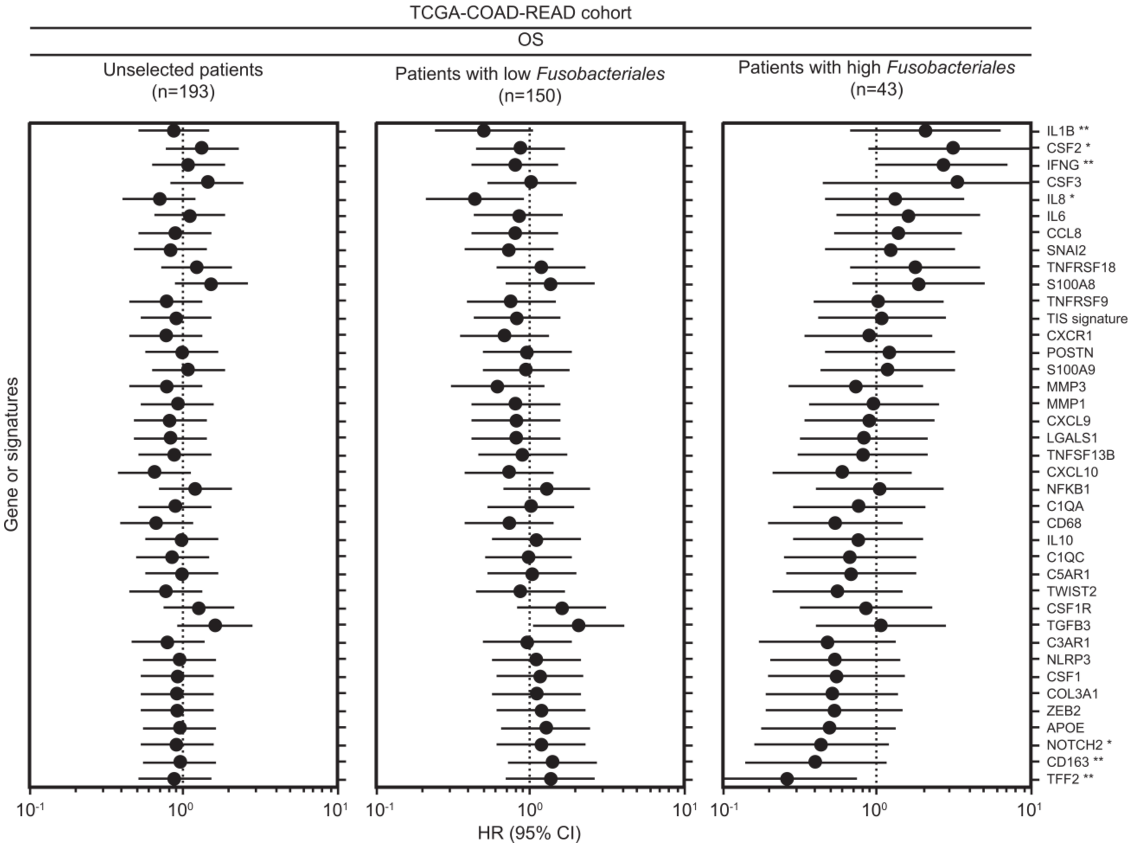

Cox regression models fitted on patients of the TCGA-COAD-READ cohort with mesenchymal tumours (either CMS4 and/or CRIS-B) for each gene/signature identified from analysis presented in **Fig. 6A**. Patients were classified as *Fusobacteriales*-low or high using the corresponding 75th percentile relative abundance (RA) as cut-off. Univariate Cox regression models were fitted when evaluating association between *Fusobacteriales* (high vs. low; reference low) and OS in the whole unselected patient population (left panel). Cox regression models with an interaction term between *Fusobacteriales* (high vs. low; reference low) and gene/signature (high vs. low, reference low) and OS were fitted to evaluate differential impact of gene/signature on clinical outcome by

Transcriptomic-dependent *Fn/Fusobacteriales* impact.

Fusobacteriales (right panels). * and ** denote interaction P-values lower than 0.05 and lower than or equal to 0.1, respectively.

Transcriptomic-dependent *Fn/Fusobacteriales* impact.

Supplementary Figure 13.

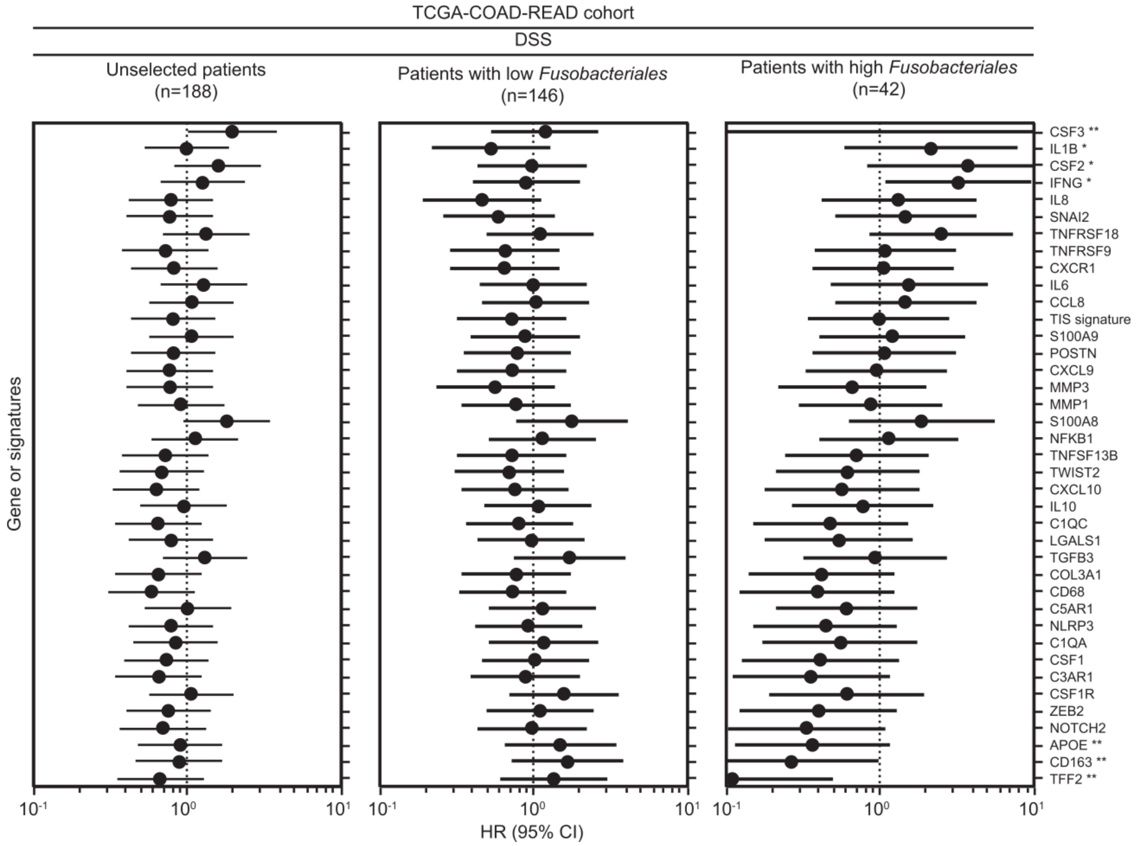

Cox regression models fitted on patients of the TCGA-COAD-READ cohort with mesenchymal tumours (either CMS4 and/or CRIS-B) for each gene/signature identified from analysis presented in **Fig. 6A**. Patients were classified as *Fusobacteriales*-low or high using the corresponding 75th percentile relative abundance (RA) as cut-off. Univariate Cox regression models were fitted when evaluating association between *Fusobacteriales* (high vs. low; reference low) and DSS in the whole unselected patient population (left panel). Cox regression models with an interaction term between *Fusobacteriales* (high vs. low; reference low) and gene/signature (high vs. low, reference low) and DSS were fitted to evaluate differential impact of gene/signature on clinical outcome by

Transcriptomic-dependent *Fn/Fusobacteriales* impact.

Fusobacteriales (right panels). * and ** denote interaction P-values lower than 0.05 and lower than or equal to 0.1, respectively.

Transcriptomic-dependent *Fn/Fusobacteriales* impact.

Supplementary Figure 14.

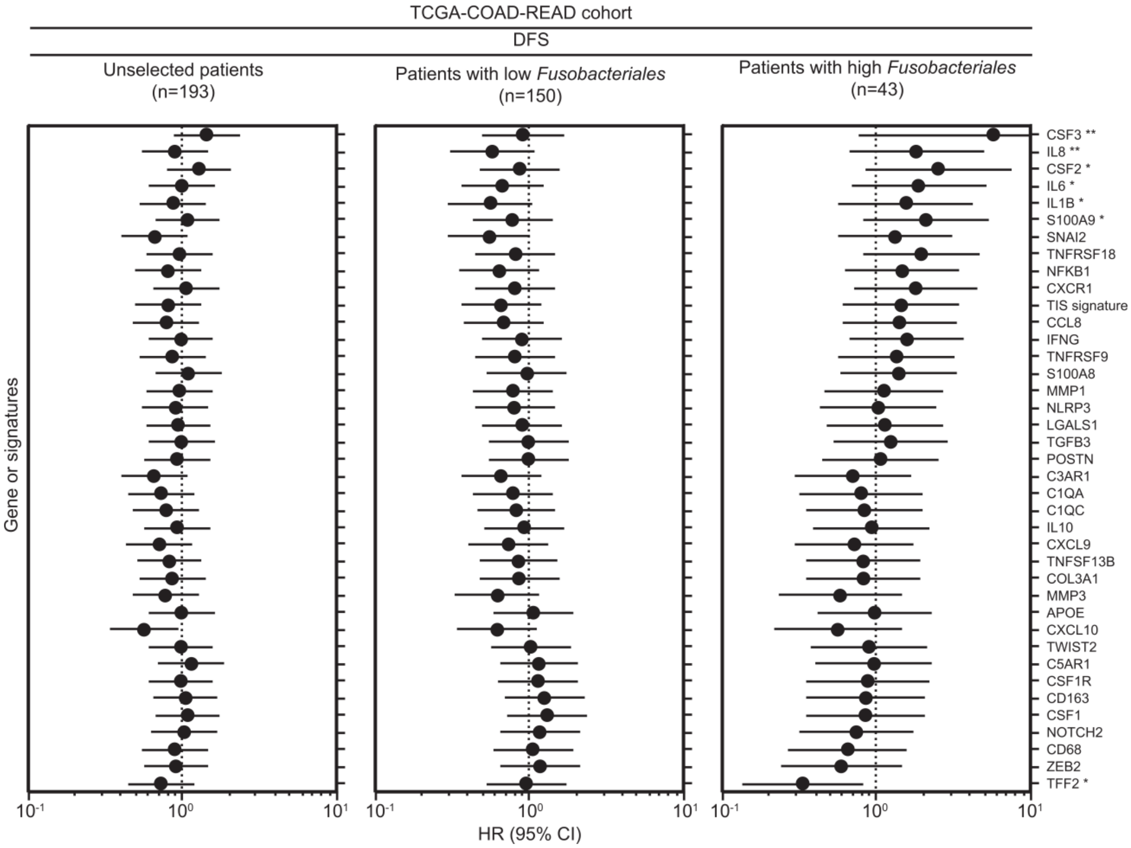

Cox regression models fitted on patients of the TCGA-COAD-READ cohort with mesenchymal tumours (either CMS4 and/or CRIS-B) for each gene/signature identified from analysis presented in **Fig. 6A**. Patients were classified as *Fusobacteriales*-low or high using the corresponding 75th percentile relative abundance (RA) as cut-off. Univariate Cox regression models were fitted when evaluating association between *Fusobacteriales* (high vs. low; reference low) and DFS in the whole unselected patient population (left panel). Cox regression models with an interaction term between *Fusobacteriales* (high vs. low; reference low) and gene/signature (high vs. low, reference low) and DFS were fitted to evaluate differential impact of gene/signature on clinical outcome by

Transcriptomic-dependent *Fn/Fusobacteriales* impact.

Fusobacteriales (right panels). * and ** denote interaction P-values lower than 0.05 and lower than or equal to 0.1, respectively.

Captions for Supplementary Tables for “Patients with mesenchymal tumours and high *Fusobacteriales* prevalence have worse prognosis in colorectal cancer (CRC)”

Manuela Salvucci[1], Nyree Crawford[2], Katie Stott[2], Susan Bullman[3,4], Daniel B. Longley[2], and Jochen H.M. Prehn[1]*

[1]Centre for Systems Medicine, Department of Physiology and Medical Physics, Royal College of Surgeons in Ireland, Dublin, Ireland;

[2]Patrick G. Johnston Centre for Cancer Research, School of Medicine, Dentistry and Biomedical Science, Queen’s University Belfast, Northern Ireland, UK;

[3]Dana-Farber Cancer Institute, Harvard Medical School, Boston, USA;

[4]Fred Hutchinson Cancer Research Center, Human Biology Division, Seattle, USA.

Corresponding author: Prof. Jochen H. M. Prehn, Department of Physiology and Medical Physics, Royal College of Surgeons in Ireland, 123 St. Stephen’s Green, Dublin 2, Ireland. Tel.: +353-1-402-2255; Fax: +353-1-402-2447; E-mail: jprehn@rcsi.ie.

Data and code availability: Datasets and source code will be publicly available and archived upon publication at Zenodo (https://10.5281/zenodo.4019142).

Supplementary Table 1.

Clinico-pathological and demographic characteristics of the CRC patients included in this study ("Overall") and grouped by cohort, namely "in house Taxonomy" and "TCGA-COAD-READ". For continuous variables, median, interquartile range, and statistical significance (P-value) determined by Kruskal-Wallis tests are reported. For categorical values, number, and percentage of cases by level and statistical significance (P-value) determined by χ^2 tests are reported.

Supplementary Table 2.

Patient-level bacterium data for cases of the Taxonomy and TCGA-COAD-READ cohort. *Fn* load measured by qPCR for patients of the Taxonomy cohort is available in the sheet "Taxonomy cohort (n=140)". Relative abundance of *Fusobacteriales* and higher resolution taxonomic ranks (family, genus and species) including the *Fn* species for the patients in the TCGA-COAD-READ cohort is available in the sheet "TCGA-COAD-READ cohort (n=605)". For the TCGA-COAD-READ cohort, genuses/species with an average relative abundance lower than 0.05 were aggregated as "Other".

Supplementary Table 3.

Association between mutational status and *Fusobacteriales* relative abundance in the TCGA-COAD-READ patients. Statistical significance was assessed by χ^2 independence tests and χ^2 statistics, unadjusted- and FDR-corrected mod-likelihood P-values are reported for each mutation that was either selected *a priori* or was found to be statistically significant altered when comparing *Fusobacteriales*-low vs. -high patients (75th percentile cut-off) of the TCGA-COAD-READ cohort.

Supplementary Table 4.

Association between recurrent copy number aberrations identified by GISTIC analysis when comparing *Fusobacteriales*-low vs. -high patients (75th percentile cut-off) of the TCGA-COAD-READ cohort.

Supplementary Table 5.

Association between gene expression profiles and *Fusobacteriales* relative abundance in the TCGA-COAD-READ patients was assessed by Spearman correlation. Correlation coefficient R, corresponding 95% confidence intervals, unadjusted- and FDR-corrected P-values are reported for each protein that was found to be statistically significant altered in the TCGA-COAD-READ cohort.

Supplementary Table 6.

Association between protein expression profiles and *Fusobacteriales* relative abundance in the TCGA-COAD-READ patients was assessed by Spearman correlation. Correlation coefficient R, corresponding 95% confidence intervals, unadjusted- and FDR-corrected P-values are reported for each protein that was found to be statistically significant altered in the TCGA-COAD-READ cohort.

Supplementary Table 7.

Un-adjusted and adjusted Cox regression models for patients of the TCGA-COAD-READ cohort. Cox regression models were fitted with an interaction term between *Fusobacteriales* (high vs. low, using the 75th percentile relative abundance as cut-off) and mesenchymal status (mesenchymal vs. non-mesenchymal). Adjusted model 1 and 2 were fitted including precision variables. Model 1 used as adjustment covariates key clinical-pathological characteristics, namely age (continuous), stage (categorical, I to IV), tumour location (categorical, colon vs. rectum) and sex (categorical, male vs. female). Model 2 used as adjustment covariates a more extensive set (i. e. super-set) of clinico-pathological characteristics additionally including history of colon polyps (categorical, yes vs. no) and history of other malignancy as comorbidities.

Supplementary Table 8.

Detailed statistical output (coefficients and P-values) of logistic models 1 (*Fusobacteriales~gene/signature*) and 2 (*Fusobacteriales~gene/signature:molecular subtype*) fitted for a set of hypothesis-driven gene/signature profiles in patients of the TCGA-COAD-READ cohort presented in **Fig. 6A**. Table include all genes/signatures tested (regardless of statistical significance) reported in ascending order of interaction P-values from model 2 determined in the TCGA-COAD-READ cohort (discovery cohort). For completeness, detailed statistical output is also reported for the Taxonomy cohort.

Supplementary Materials and Methods for “Patients with mesenchymal tumours and high *Fusobacteriales* prevalence have worse prognosis in colorectal cancer (CRC)”

Manuela Salvucci[1], Nyree Crawford[2], Katie Stott[2], Susan Bullman[3,4], Daniel B. Longley[2], and Jochen H.M. Prehn[1]*

[1]Centre for Systems Medicine, Department of Physiology and Medical Physics, Royal College of Surgeons in Ireland, Dublin, Ireland;

[2]Patrick G. Johnston Centre for Cancer Research, School of Medicine, Dentistry and Biomedical Science, Queen’s University Belfast, Northern Ireland, UK;

[3]Dana-Farber Cancer Institute, Harvard Medical School, Boston, USA;

[4]Fred Hutchinson Cancer Research Center, Human Biology Division, Seattle, USA.

Corresponding author: Prof. Jochen H. M. Prehn, Department of Physiology and Medical Physics, Royal College of Surgeons in Ireland, 123 St. Stephen’s Green, Dublin 2, Ireland. Tel.: +353-1-402-2255; Fax: +353-1-402-2447; E-mail: jprehn@rcsi.ie.

Data and code availability: Datasets and source code will be publicly available and archived upon publication at Zenodo (https://10.5281/zenodo.4019142).

Contents

Transcriptomic-dependent *Fn/Fusobacteriales* impact.

In vitro experiments

Cell culture

HCT116 and HT29 cells were purchased as authenticated stocks from ATCC (Teddington, UK). HT29 cells were cultured in DMEM medium (ThermoFisher Scientific Inc.) supplemented with 10% fetal bovine serum (Invitrogen, Paisley, UK). HCT116 cells were cultured in McCoys 5A medium (ThermoFisher Scientific Inc.) supplemented with 10% fetal bovine serum (Invitrogen, Paisley, UK). Cell lines were screened for the presence of mycoplasma utilising MycoAlert Mycoplasma Detection Kit (Lonza) monthly and cultured for no more than 20 passages.

Fn culturing conditions

Fusobacterium nucleatum subsp. *nucleatum* strain 25586 was purchased from American Type Culture Collection (ATCC, Middlesex, UK). *Fn* was cultured at 37ºC under anaerobic conditions (DG250, Don Whitley Scientific, West Yorkshire, UK) in Fastidious Anaerobic Broth (Neogen, formerly Lab M, Scotland, UK).

Co-culture experiments

HT29 and HCT116 cells were co-cultured with *Fn* at a Multiplicity of Infection (MOI) of 10:1, 100:1 and 1000:1 under normal culturing conditions for the CRC cell lines.

Western Blotting

Western blotting analysis was carried out as previously described [1]. IκBα antibody (#9242) was supplied by Cell Signaling Technology (Danvers, MA) and β-actin (#A5316) was supplied by Sigma.

Transcriptomic-dependent *Fn/Fusobacteriales* impact.

NFκB activity assay

Cells were co-transfected with NFκB luciferase reporter and Renilla constructs using X-tremeGENE HP (Promega, Madison, WI), as previously described [2]. Cells were lysed with Passive Lysis Buffer (Promega, Madison, WI) and Luciferase and Renilla activity assessed by luminescence using D-Luciferin and Colenterazine as substrates.

Quantitative polymerase chain reaction (qPCR)

RNA was extracted, according to manufacturer's instructions using the High Pure RNA Isolation kit (Roche, Burgess Hill, UK). The Transcriptor First Strand cDNA synthesis kit (Roche, Burgess Hill, UK) was utilized to synthesize cDNA, according to manufacturer's instructions. qPCR was performed on the LC480 light cycler, using Syber green, according to manufacturer's instructions. Primer sequences:

- **TNFα F**: CAGCCTCTTCTCCTTCCTGAT;
- **TNFα R**: GCCAGAGGGCTGATTAGAGA;
- **β-tubulin F**: CGCAGAAGAGGAGGAGGATT;
- **β-tubulin R**: GAGGAAAGGGGCAGTTGAGT.

Association between *Fusobacteriales* and *Fn* prevalence in tumour resections with host characteristics in CRC

Clinical cohorts

In this study, we profiled *Fusobacteriales* and/or *Fn* in primary tumour tissue resections from n=645 CRC patients from an in-house (Taxonomy, [3-4]) and a public protected dataset (The

Cancer Genome Atlas, TCGA-COAD-READ). Demographic and clinical and pathological characteristics of the two cohorts are compared and contrasted in **Suppl. Table 1**, which was generated with the *python* package *TableOne* [5].

Taxonomy cohort

Stage II and III colorectal patients (n=156) from a multi-centre study (St Vincent's Hospital, Dublin, IE; University Hospital Vall d'Hebron, Barcelona, ES; University of Aberdeen, UK; University of Florence, IT) were accrued, as previously described (Taxonomy cohort, [3]). The cohort collection was approved by the Medicine, Dentistry, and Biomedical Sciences School Ethics Committee (ref: 12/12v4), as previously described [3]. In downstream analyses, we included patients with available gene expression profiling (Almac Xcel array, Almac Diagnostics, Craigavon, UK, GSE103479, [3-4]) and estimation of *Fn* load from resected tumour tissue (at least 50% tumour content) by qPCR (n=140). The primary outcome for the Taxonomy cohort was overall survival (OS), but disease-free survival (DFS) records were also available.

TCGA COAD-READ cohorts

Stage I to IV patients with cancer of the colon (COAD) or rectum (READ) accrued by The Cancer Genome Atlas (TCGA) network with available fresh frozen tumour resections of sufficient quality and quantity for sequencing analysis (https://www.cancer.gov/about-nci/organization/ccg/research/structural-genomics/tcga/studied-cancers) were considered for inclusion in the study (n=629). In downstream analyses, we included all patients (n=605) that i) where not listed as "Redacted" in the clinical metadata retrieved from Liu *et al.* [6]; and ii) had at least a high quality RNASeq experiment from primary tumour from which bacterial relative abundance could be estimated **(Supplementary Materials and Methods Figure 1**).

Transcriptomic-dependent *Fn/Fusobacteriales* impact.

Throughout this study we investigated the relationship between the relative abundance of *Fusobacteriales* and higher resolution taxonomic ranks, including the *Fn* species, and characteristics of the host using several signatures and *-omic* views, namely mutations, copy number aberrations, gene and protein expression, (described in detail in the following sections). **Supplementary Materials and Methods Fig. 2** depicts data (cross-)availability and highlights what set of patients was included in each analysis.

Transcriptomic-dependent *Fn/Fusobacteriales* impact.

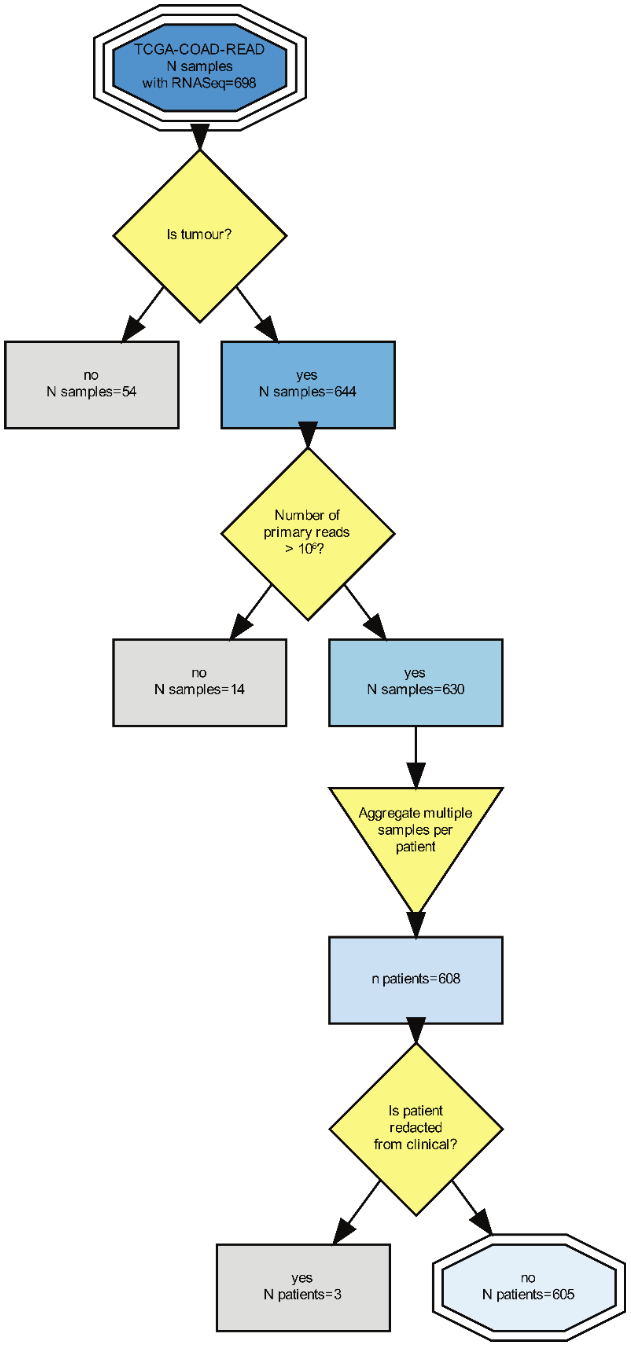

Supplementary Materials and Methods Figure 1. Flowchart depicting inclusion criteria with corresponding number of samples/patients available in the TCGA-COAD-READ cohort at each step of the analysis.

Transcriptomic-dependent *Fn/Fusobacteriales* impact.

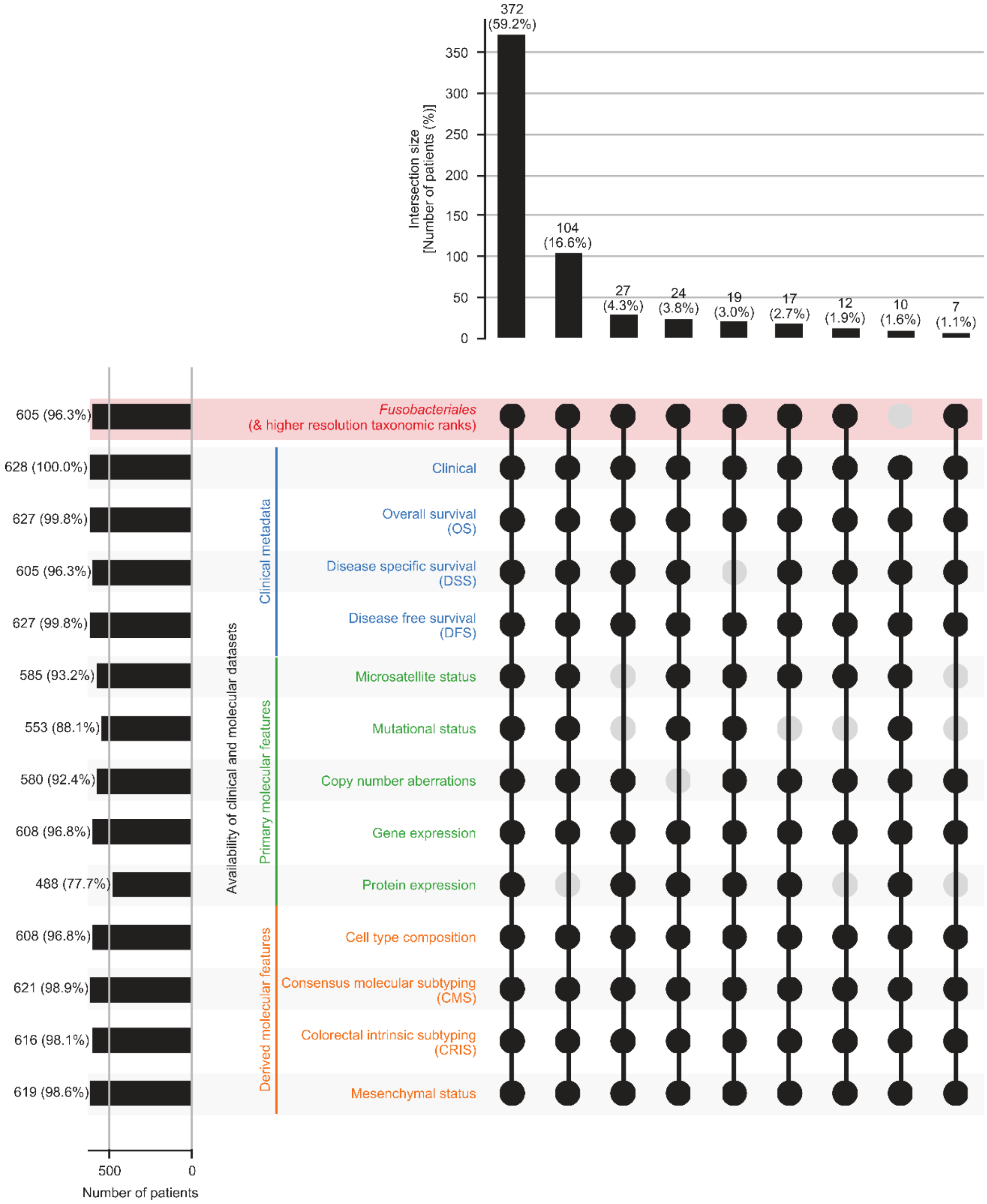

Supplementary Materials and Methods Figure 2. (Cross-)availability of *Fusobacteriales* estimates (and higher resolution taxonomic ranks, including the *Fn* species), clinical and primary and derived *-omic* data for the TCGA-COAD-READ patients included in this study.

Determination of *Fn* load and *Fusobacteriales* relative abundance in tumour resections of CRC patients

Taxonomy cohort

Fn abundance was quantified through qPCR analysis from tumour DNA, performed on the Roche Light Cycler 480 Real Time PCR Instrument (Roche, Burgess Hill, UK), using Syber green, according to manufacturer's instructions. Each reaction contained 80 ng of genomic DNA which was assessed in duplicate, in 25 µl reactions. The abundance of *Fn* DNA in each tumour sample was normalised to the human reference gene Prostaglandin transporter (PGT) using the $2^{-\Delta Ct}$ method, where ΔCt = Ct value for *Fn* – Ct value for PGT. Primer sequences:

- ***Fn* F**: CAACCATTACTTTAACTCTACCATGTTCA;
- ***Fn* R**: GTTGACTTTACAGAAGGAGATTATGTAAAAATC;
- **PGT F**: ATCCCCAAAGCACCTGGTTT;
- **PGT R**: AGAGGCCAAGATAGTCCTGGTAA.

TCGA-COAD-READ cohort

Fusobacteriales relative abundance in primary tumour specimens was estimated from RNASeq using a subtractive method implemented by the *PathSeq* pipeline (version 2, *PathSeqPipelineSpark* routine, [7-8]), powered by the Genome Analysis Toolkit engine (GATK, https://gatk.broadinstitute.org/, [9]) and the Apache Spark framework. Level 1 protected BAM sequencing files from RNASeq experiments for all TCGA-COAD-READ patients were accessed via the GDC Data Portal (https://portal.gdc.cancer.gov/) and served as input to the pipeline. Briefly, host reads (i.e. human) were filtered out and the remaining unmapped reads were aligned to microbial reads based on reference taxonomies for bacteria, fungi and viruses using a (default) min-clipped-read-length of 31. Host and microbe references files were retrieved from the GATK Resource Bundle (ftp://gsapubftp-anonymous@ftp.broadinstitute.org/bundle/pathseq/). We ran the *PathSeq* pipeline on n=698 patient samples of which n=644 were from tumour tissue. We restricted the analysis to samples which exceeded 10 million primary reads, resulting in n=630 high quality tumour samples for downstream analysis. Next, we collapsed microbial relative abundance from multiple samples and multiple tissue types (primary, recurrent and metastatic) of the same patient by mean. In downstream analyses, we included only patients with samples resected from primary tumours (n=605). We reported relative abundance for *Fusobacteriales* at the order, family, genus and species taxonomic rank as normalized score expressed as percentage of the total relative abundance of the bacterial kingdom. Some of the species, denoted by the suffix "_sp", such as *Fusobacterium_sp._CM1*, reported by *PathSeq* are sub-species/strains. This may lead to under-reporting the relative abundance of e. g. *Fusobacterium nucleatum* as it does not include the abundances of its sub-species/strains. To avoid this issue, we manually re-mapped sub-species/strains to their parent species by blasting their sequence in NCBI (https://www.ncbi.nlm.nih.gov/nuccore/). We performed the re-mapping only when the percentage of identity between the sub-species/strain and its parent species exceeded 97%, as indicated in **Supplementary Materials and Methods Table 1**. The majority of the sub-species/strains mapped to *Fn*.

Transcriptomic-dependent *Fn/Fusobacteriales* impact.

Supplementary Materials and Methods Table 1. Sub-species/strain mapping to parent species.

Sub-species/strain	Candidate parent species	Per. identity	Remapped parent species
Cetobacterium_sp._ZOR0034	Cetobacterium_somerae	100%	Cetobacterium_somerae
Cetobacterium_sp._ZWU0022	Cetobacterium_somerae	99.78%	Cetobacterium_somerae
Fusobacterium_sp._CM1	Fusobacterium_nucleatum	99.86%	Fusobacterium_nucleatum
Fusobacterium_sp._CM21	Fusobacterium_nucleatum	99.86%	Fusobacterium_nucleatum
Fusobacterium_sp._CM22	Fusobacterium_nucleatum	99.70%	Fusobacterium_nucleatum
Fusobacterium_sp._HMSC064B11	Fusobacterium_nucleatum	99.93%	Fusobacterium_nucleatum
Fusobacterium_sp._HMSC064B12	Fusobacterium_nucleatum	99.82%	Fusobacterium_nucleatum
Fusobacterium_sp._HMSC065F01	Fusobacterium_nucleatum	99.87%	Fusobacterium_nucleatum
Fusobacterium_sp._OBRC1	Fusobacterium_nucleatum	100%	Fusobacterium_nucleatum
Fusobacterium_sp._HMSC073F01	Fusobacterium_varium	100%	Fusobacterium_varium
Leptotrichia_sp._Marseille-P3007	Leptotrichia_buccalis	98.37%	Leptotrichia_buccalis
Leptotrichia_sp._oral_taxon_225	Leptotrichia_trevisanii	99.52%	Leptotrichia_trevisanii
Leptotrichia_sp._oral_taxon_879	Leptotrichia_hongkongensis?	96.86%	un-mapped
Leptotrichia_sp._oral_taxon_212	Leptotrichia_hongkongensis?	92.67%	un-mapped
Leptotrichia_sp._oral_taxon_847	Leptotrichia_massiliensis?	92.04%	un-mapped
Leptotrichia_sp._oral_taxon_215	No candidate parent species found	un-mapped	
Fusobacterium_sp._oral_taxon_370	Fusobacterium_nucleatum or Fusobacterium_periodonticum?	95.33% for both	un-mapped

Gene expression analysis

For the Taxonomy cohort, transcriptomics data (Almac Xcel array, Almac Diagnostics, Craigavon, UK; GSE103479) were processed as previously described [3-4]. For the TCGA-COAD-READ cohort, level 4 batch-corrected and normalised gene expression profiles by RNASeq were retrieved from the TCGA PanCanAtlas data-freeze release (*EBPlusPlusAdjustPANCAN_IlluminaHiSeq_RNASeqV2.geneExp.tsv*) from https://gdc.cancer.gov/about-data/publications/pancanatlas).

Transcriptomic-based signatures

We reviewed the literature and selected signatures encoding signalling pathways of interest including:

Transcriptomic-dependent *Fn/Fusobacteriales* impact.

- **proliferation**: mean gene expression of BIRC5, CCNB1, CDC20, NUF2, CEP55, NDC80, MKI67, PTTG1, RRM2, TYMS, and UBE2C ([10]).
- **epithelial-to-mesenchymal transition (EMT)**: difference in gene expression of epithelial (CDH1, DSP, OCLN) and mesenchymal (VIM, CDH2, FOXC2, SNAI1, SNAI2, TWIST1, FN1, ITGB6, MMP2, MMP3, MMP9, SOX10, GCS) genes ([11]).
- **metastasis**: difference in gene expression of markers promoting (SNRPF, EIF4EL3, HNRPAB, DHPS, PTTG1, COL1A1, COL1A2, and LMNB1) and inhibiting (ACTG2, MYLK, MYH11, CNN1, HLA-DPB1, RUNX1, MT3, NR4A1, and RBM5) metastasis ([12]).
- **DNA damage**: mean gene expression of PRKDC, NEIL3, FANCD2, BRCA2, EXO1, XRCC2, RFC4, USP1, UBE2T, and FAAP24 ([13]).
- **WNT signalling**: mean gene expression of AC023512.1, APC, APC2, AXIN1, AXIN2, BTRC, CACYBP, CAMK2A, CAMK2B, CAMK2D, CAMK2G, CCND1, CCND2, CCND3, CER1, CHD8, CHP1, CHP2, CREBBP, CSNK1A1, CSNK1A1L, CSNK1E, CSNK2A1, CSNK2A2, CSNK2B, CTBP1, CTBP2, CTNNB1, CTNNBIP1, CUL1, CXXC4, DAAM1, DAAM2, DKK1, DKK2, DKK4, DVL1, DVL2, DVL3, EP300, FBXW11, FOSL1, FRAT1, FRAT2, FZD1, FZD10, FZD2, FZD3, FZD4, FZD5, FZD6, FZD7, FZD8, FZD9, GSK3B, JUN, LEF1, LRP5, LRP6, MAP3K7, MAPK10, MAPK8, MAPK9, MMP7, MYC, NFAT5, NFATC1, NFATC2, NFATC3, NFATC4, NKD1, NKD2, NLK, PLCB1, PLCB2, PLCB3, PLCB4, PORCN, PPARD, PPP2CA, PPP2CB, PPP2R1A, PPP2R1B, PPP2R5A, PPP2R5B, PPP2R5C, PPP2R5D, PPP2R5E, PPP3CA, PPP3CB, PPP3CC, PPP3R1, PPP3R2, PRICKLE1, PRICKLE2, PRKACA, PRKACB, PRKACG, PRKCA, PRKCB, PRKCG, PRKX, PSEN1, RAC1, RAC2, RAC3, RBX1, RHOA,

ROCK1, ROCK2, RUVBL1, SENP2, SFRP1, SFRP2, SFRP4, SFRP5, SIAH1, SKP1, SMAD2, SMAD3, SMAD4, SOX17, TBL1X, TBL1XR1, TBL1Y, TCF7, TCF7L1, TCF7L2, TP53, VANGL1, VANGL2, WIF1, WNT1, WNT10A, WNT10B, WNT11, WNT16, WNT2, WNT2B, WNT3, WNT3A, WNT4, WNT5A, WNT5B, WNT6, WNT7A, WNT7B, WNT8A (https://www.gsea-msigdb.org/gsea/msigdb/cards/KEGG_WNT_SIGNALING_PATHWAY).

- **Tumour Inflammation Signature (TIS)**: mean gene expression of CD276, HLA-DQA1, CD274, IDO1, HLA-DRB1, HLA-E, CMKLR1, PDCD1LG2, PSMB10, LAG3, CXCL9, STAT1, CD8A, CCL5, NKG7, TIGIT, CD27, and CXCR6 ([14]).
- **Cytolytic activity**: mean gene expression of GZMA, and PRF1 ([15]).
- **Interferon gamma (IFNγ)**: mean expression of IFNG, LAG3, CXCL9, and CD274 ([16]).

For both cohorts, we applied a robust scaling transformation (*sklearn.preprocessing.RobustScaler*) prior to computing the signatures. For the TCGA-COAD-READ cohort, gene expression profiles were quantile transformed (*sklearn.preprocessing.QuantileTransformer*) with the *output_distribution* flag set to *normal* prior to robust scaling.

Markers for pro- and anti-inflammatory processes

We selected NFKB1, TNF, IL6 and IL8 as key inflammatory markers to include in the analysis presented in **Fig. 4G-H**. Additionally, we performed a literature search and identified markers specific for pro- [17] and anti-inflammation [18] processes to further include in our analysis (**Fig. 4G-H**).

Transcriptomic-dependent *Fn/Fusobacteriales* impact.

Characterization of the tumour microenvironment

Cell type composition was computationally deconvoluted from bulk tumour gene expression data using 2 methods: *Microenvironment Cell Populations-counter* (MCP-counter, [19]); and *quantification of the Tumor Immune contexture from human RNA-seq data* (quanTIseq, [20]). MCP-counter, implemented as *R* package, uses marker genes to estimate the abundance (in arbitrary units) of endothelial cells, fibroblasts and 8 immune cell types including T cells, CD8$^+$ T cells, cytotoxic lymphocytes, B lineage, natural killer (NK) cells, monocytic lineage, myeloid dendritic cells and neutrophils. For the Taxonomy cohort, we computed MCP-counter estimates as previously reported [4] and we normalized the resulting scores using a robust scaler (*sklearn.preprocessing.RobustScaler*). For the TCGA-COAD-READ cohort, we applied a quantile-transform (*sklearn.preprocessing.QuantileTransformer* with optimal distribution set to normal) followed by robust scaling (*sklearn.preprocessing.RobustScaler*) prior to applying the MCP-counter algorithm. Cell type composition was further characterized by applying the quanTIseq pipeline (step 3 in *quanTIseq_pipeline.sh* from https://icbi.i-med.ac.at/software/quantiseq/doc/downloads/quanTIseq_pipeline.sh) to gene expression profiles of the Taxonomy ([4], flag set to account for the microarray nature of the data) or TCGA-COAD-READ cohort (*EBPlusPlusAdjustPANCAN_IlluminaHiSeq_RNASeqV2.geneExp.tsv*) without any additional pre-processing transformation. The quanTIseq algorithm uses a signature matrix to determine the fraction of tumour and stromal cells along with 10 immune cell types including non-regulatory CD4$^+$ T cells, CD8$^+$ T cells, regulatory T cells, dendritic cells, B cells, NK cells, neutrophils, monocytes, and classically- (M1) and alternatively- (M2) activated macrophages.

Patients' classification into transcriptomic-based molecular subtypes

Patients' tumour samples were classified according to the *Consensus Molecular Subtype* (CMS, [21]) and *Cancer Intrinsic Subtype* (CRIS, [22]).

Circa 20% of primary tumour samples cannot be classified as CMS1 to CMS4 and they are marked as "no label" (NOLBL, [21]). In order to maximize the number of patients with CMS assignments, patients were classified in CMS groups using the nearest prediction from the random forest (RF) classifier (*R* package *CMSclassifier*, https://github.com/Sage-Bionetworks/CMSclassifier, [21]). For the Taxonomy cohort, we used the labels previously reported by McCorry *et al.* [4]. Similarly, for the TCGA-COAD-READ cohort, we retrieved the RF nearest prediction labels provided by Guinney *et al.* ([21], *cms_labels_public_all.txt* from synapse #: syn4978511). Additionally, we computed nearest prediction RF labels for the whole TCGA-COAD-READ cohort *de novo* to classify patients. We additionally included the CMS assignments for those patients that had not been subtyped as part of the Guinney *et al.* study. For both cohorts, subtype assignments mapping to multiple CMS classes were classified as indetermined and, thus, set to NOLBL.

Patients were subjected to CRIS subtyping and labelled as CRIS-A to CRIS-E or NOLBL (if Benjamini-Hochberg–corrected false discovery rate (BH.FDR) exceeded 0.2), as described in Isella *et al.* [22]. For the Taxonomy cohort, CRIS subtyping was performed using the nearest template prediction (NTP) classifier, available from GenePattern (https://genepattern.broadinstitute.org/gp/pages/login.jsf) as reported by McCorry *et al.* [4]. For the TCGA-COAD-READ cohort, we apply the CRIS subtyping to the whole TCGA-COAD-READ cohort. For the final CRIS assignments, we included either the labels provided from the

Isella *et al.* publication [22] or the labels we computed *de novo* for patients that had not been subtyped as part of the original study.

Unbiased and systematic analysis of human host associations with *Fusobacteriales* in the TCGA-COAD-READ cohort

Mutational status.

Genomic intra-tumour heterogeneity and mutational burden expressed as number of silent and non-silent mutations per Mb was retrieved from the supplementary materials of Thorsson *et al.* [23] and corresponding data-freeze (*mutation-load_updated.txt* from https://gdc.cancer.gov/about-data/publications/panimmune), respectively. Patients were classified as microsatellite stable (MSS) or unstable (MSI) using a cut-off of 0.4 applied to the MANTIS score retrieved from the supplementary materials of Bonneville *et al.* [24].

Somatic mutation data in Mutation Annotation Format (MAF, *mc3.v0.2.8.PUBLIC.maf.gz*) were retrieved from the TCGA PanCanAtlas data-freeze release (https://gdc.cancer.gov/about-data/publications/pancanatlas) and restricted to the subset of patients diagnosed with COAD-READ cancers. We used the *maftools R* package (version 2.2.10, [25]) to compute conversion changes (C>A, C>G, C>T, T>C, T>A, T>G) and the percentage of transitions (Ti) and transversions (Tv) from the MAF file.

For each patient and each gene, we extracted from the MAF file the number of detected mutational aberrations. As aberrations, we included frame shift deletions and insertions, in frame deletions and insertions, missense and nonsense mutations and splice sites and we excluded the following variants: 3' flank, 3' UTR, 5' flank, 5' UTR, Intron, RNA, silent and non-stop mutations.

Transcriptomic-dependent *Fn/Fusobacteriales* impact.

Association between *Fusobacteriales* relative abundance (low vs. high using 75th percentile as cut-off) and mutational status (number of aberrations) was assessed with χ^2 independence tests. We restricted the analysis to genes with aberrations in at least 5% of patients (n=818 genes out of 21332, ~4%). We reported mod-log-likelihood P-values, adjusted for multiple comparisons with Benjamini-Hochberg FDR correction (**Fig. 3C-D** and **Suppl. Table 3**). Similarly, association between *Fn* and mutational status was assessed with χ^2 independence tests in the TCGA-COAD-READ and Taxonomy cohorts (**Suppl. Fig. 3**). *Fn* refers to either relative abundance or load for the TCGA-COAD-READ and Taxonomy cohorts, respectively. Patients of the TCGA-COAD-READ cohort were considered wild-type for the gene of interest if the number of considered aberrations was null, mutant otherwise. Assessment of mutational status in the Taxonomy cohort has been previously described [3].

Copy number alterations (CNAs)

Copy number alterations (*broad.mit.edu_PANCAN_Genome_Wide_SNP_6_whitelisted.seg*) were retrieved from the TCGA PanCanAtlas data-freeze release (https://gdc.cancer.gov/about-data/publications/pancanatlas). Recurrent CNAs were identified in the TCGA PanCancer collection via The Genomic Identification of Significant Targets In Cancer (GISTIC, version 2, [26]) using a cut-off q-value of 0.25 and confidence threshold of 0.90 for peak boundaries (**Suppl. Fig. 5**). A region was classified as amplification or deletion if the LogR was above or below the 0.1 threshold. Downstream analyses were restricted to patients from the TCGA-COAD-READ cohort with *Fusobacteriales* estimates (n=563). Copy number aberrations were visualised as a heatmap using the *python* package *CNVkit* (version 0.9.7, function *do_heatmap*), (**Fig. 3E**). Percentage of patients with aberrations at a given genomic position were visualised with the *R* package *copynumber* (version 1.26.0, function *plotFreq*, [27]), (**Sup. Fig. 6**).

Transcriptomic-dependent *Fn/Fusobacteriales* impact.

Differences in copy number aberrations at the cytoband level were computed by computing the difference in mean lesion frequency between patients with high vs. low *Fusobacteriales* relative abundance (75th percentile cut-off), (**Fig. 3F**). Top 3 differential copy number aberrations at the cytoband level were visualised in **Fig. 3G**.

Aberrations in transcriptional and protein profiles

A systematic screen was carried out to identify aberrations in transcriptional and protein profiles by *Fusobacteriales* relative abundance in patients of the TCGA-COAD-READ cohort. Association between *Fusobacteriales* relative abundance and either gene or protein expression was assessed by Spearman correlation (function *pairwise_corr)* from the *python* package *pingouin* (version 0.3.11, [28]). P-values were adjusted for multiple comparisons for False Discovery Rate with Benjamini-Hochberg (function *pingouin.multicomp* from the python package *pingouin*). For transcriptional profiles, we restricted the analysis to the 5000 most variant genes. All available proteins were tested (n=189 proteins). Genes and proteins whose expression differed by *Fusobacteriales* relative abundance were put forward for pathway enrichment analyses carried out with the *gseapy* package (version 0.10.2, [29]) which provides a wrapper (function *gseapy.enrichr*) for *EnrichR* [30-31], (**Fig. 3 H-I, K-L** and **Sup. Fig.7-8**).

Exploration of putative mechanisms underlying differential impact of *Fn/Fusobacteriales* prevalence by tumour biology

We fitted 2 logistic regression models to identify putative mechanisms underlying the differential impact of *Fn/Fusobacteriales* prevalence in mesenchymal vs. non-mesenchymal tumours. Specifically, we fitted:

- **model 1**: univariate logistic regression model (*Fusobacteriales ~ gene/signature*);

Transcriptomic-dependent *Fn/Fusobacteriales* impact.

- **model 2**: logistic regression model with an interaction term for mesenchymal status (*Fusobacteriales ~ gene/signature * mesenchymal status*).

Patients were grouped into *Fusobacteriales*-low vs. high using the 75th percentile of *Fusobacteriales* relative abundance as cut-off. Selection of gene expression or signatures to include in model evaluation was hypothesis driven and this analysis was considered exploratory in nature. Thus, no P-value adjustment for multiple comparisons was performed. Tumour mesenchymal status was treated as binary (yes, no). Tumour were classed as mesenchymal if they were classified as CMS4 and/or CRIS-B based on transcriptomic assignments from the CMS [21] and/or CRIS [22] subtyping strategies. Logistic regression models were fitted using the function *statsmodels.formula.api.logit* from the *python* package *statsmodels* (version 0.11.1, [32]).

Statistical analysis.

Statistical significance was set at $P<0.05$, unless otherwise specified.

Comparative analyses

For hypothesis-driven investigations, we visualized the association between either *Fn* or *Fusobacteriales* (order) relative abundance (high vs. low) with either split violin or mosaic plots drawn with the *python* packages *matplotlib* (version 3.3.1, [33]), *seaborn* (version 0.11.0, [34]), for continuous and categorical clinical or molecular features, respectively. For hypothesis-driven analysis, we evaluated statistical significance by either non-parametric Kruskal-Wallis or χ^2 independence tests for continuous or categorical variables, respectively. Given the hypothesis-driven and exploratory nature of these analyses, the P-values were not adjusted for multiple comparisons. In contrast, in unbiased and systematic analyses (**Fig. 3**) or when specified, P-values were adjusted for False Discovery Rate with Benjamini-Hochberg FDR correction (FDR-BH).

Outcome analysis.

As outcome endpoints, we evaluated disease-free (DFS), disease-specific (DSS)and overall (OS) survival where we consider relapse, cancer-related death or death by any cause as event, respectively. For the Taxonomy cohort where the cause of death was not annotated, we assessed exclusively DFS and OS. We used Kaplan-Meier estimators and we fit univariate and interaction Cox proportional hazards regression models to evaluate survival by covariates with the *python* package *lifelines* (version 0.25.5, [35]). We assessed statistical significance with log-rank and likelihood ratio tests, respectively. Interaction Cox regression models were fitted to evaluate the cross-talk between bacterium prevalence (high vs. low using the 75th percentile as cut-off) and mesenchymal phenotypes (*mesenchymal*: either CMS4 and/or CRIS-B; vs. *non-mesenchymal*: neither CMS4 nor CRIS-B). For the Taxonomy cohort, we used *Fn* load as pathogen prevalence (**Fig. 5A, C-D** and **Sup. Fig. 9**). For the TCGA-COAD-READ cohort, we used *Fusobacteriales* relative abundance as pathogen prevalence (**Fig. 5E, G-I, K-L** and **Sup. Fig. 10**).

In additional analysis we evaluated whether our findings were robust when accounting for covariates that may represent confounders or disease modifiers (**Suppl. Table 7**). For each clinical endpoint of interest, namely OS, DSS, DFS, for the patients of the TCGA-COAD-READ cohort, we fitted 2 additional Cox regression models where in addition to the interaction term between *Fusobacteriales* and mesenchymal status we included adjustment covariates. In adjusted model 1, we included age (continuous), stage (categorical, I to IV), tumour location (categorical, colon vs. rectum) and sex (categorical, male vs. female) as key clinical, pathological and demographic covariates. We considered including resection margins (categorical, R0 vs. R1-R2) and presence of lymphovascular invasion (categorical, yes vs. no) as disease modifiers, but decided against as these covariates were missing for a high proportion of the patients. In adjusted model 2, we expand upon adjusted model 1 by also including history of colon polyps (categorical, yes vs. no) and history of other malignancy as comorbidities. However, the covariate information was not available for all the patients included in the analysis in the manuscript. Thus, for this additional analysis, we selected only patients with available covariates (~85% of those included in **Fig. 5** of the manuscript). Also, we re-fitted the unadjusted Cox regression models reported in the manuscript to aid in the interpretation of the results (**Suppl. Table 7**).

In exploratory analysis, we additionally assessed the association between clinical outcome and pathogen relative abundance at higher taxonomic resolution (family, genus and species) for patients of the TCGA-COAD-READ cohort (**Fig. 5M** and **Sup. Fig. 11**).

We evaluated whether the gene/signature identified by the analysis presented in **Fig. 6A** as candidate targets are indeed related to clinical outcome in patients of the TCGA-COAD-READ cohort with mesenchymal tumours and high *Fusobacteriales* (**Suppl. Figs. 12-14**). To this end, we restricted our analysis to patients with mesenchymal tumours and for each clinical endpoint of interest, namely OS, DSS, DFS, we fitted Cox regression models with an interaction term for *Fusobacteriales* relative abundance (low vs. high) and each of the gene/signature (low vs. high) identified as statistically significant in the analysis presented in **Fig. 6A**. **Suppl. Figs. 12-14** visualise the association between clinical outcome (OS, DSS, DFS) and each gene/signature

Transcriptomic-dependent *Fn/Fusobacteriales* impact.

across the whole unselected patient population and withing the low- and high-Fusobacteriales subgroups.

Software and libraries

Data processing and analyses were performed in *R* (version 3.6.3, [36]) and *python* (version 3.8.10, [37]). Key libraries used in this study include *pandas* (version 1.1.2, [38]), *numpy* (version 1.19.1, [39]), *sklearn* (version 0.23.1, [40]), *matplotlib* (version 3.3.1, [33]), *seaborn* (version 0.11.0, [34]), *graphviz* (version 0.14.1, [41]), *UpSetPlot* (version 0.5.0, [42]), *tableone* (version 0.7.6, [5]), *statsmodels* (version 0.11.1, [32]), *pingouin* (version 0.3.11, [28]), *gseapy* (version 0.10.2, [29]), *lifelines* (version 0.25.5, [35]). The full list of packages and their versions along with the data and code will be publicly available and archived upon publication at Zenodo (https://10.5281/zenodo.4019142).

References

1 Crawford N, Stasik I, Holohan C *et al.* SAHA overcomes flip-mediated inhibition of smac mimetic-induced apoptosis in mesothelioma. *Cell Death & Disease* 2013;**4**:e733–3. doi:10.1038/cddis.2013.258

2 Buckley NE, Haddock P, Simoes RDM *et al.* A brca1 deficient, nfkappab driven immune signal predicts good outcome in triple negative breast cancer. *Oncotarget* 2016;**7**:19884–96. doi:10.18632/oncotarget.7865

3 Allen WL, Dunne PD, McDade S *et al.* Transcriptional Subtyping and CD8 Immunohistochemistry Identifies Patients With Stage II and III Colorectal Cancer With Poor Prognosis Who Benefit From Adjuvant Chemotherapy. *JCO Precision Oncology* 2018;**44**:1–15. doi:10.1200/po.17.00241

4 McCorry AM, Loughrey MB, Longley DB *et al.* Epithelial-to-mesenchymal transition signature assessment in colorectal cancer quantifies tumour stromal content rather than true transition. *Journal of Pathology* 2018;**246**:422–6. doi:10.1002/path.5155

5 Pollard TJ, Johnson AEW, Raffa JD *et al.* Tableone: An open source python package for producing summary statistics for research papers. *JAMIA Open* 2018;**1**:26–31. doi:10.1093/jamiaopen/ooy012

6 Liu J, Lichtenberg T, Hoadley KA *et al.* An Integrated TCGA Pan-Cancer Clinical Data Resource to Drive High-Quality Survival Outcome Analytics. *Cell* 2018;**173**:400–416.e11. doi:10.1016/j.cell.2018.02.052

7 Biosciences M. Nbt.1868.Pdf. *Nature Publishing Group* 2011;**29**. doi:10.1038/nbt0511-393

Transcriptomic-dependent *Fn/Fusobacteriales* impact.

8 Walker MA, Pedamallu CS, Ojesina AI *et al.* GATK PathSeq: a customizable computational tool for the discovery and identification of microbial sequences in libraries from eukaryotic hosts. *Bioinformatics (Oxford, England)* 2018;**34**:4287–9. doi:10.1093/bioinformatics/bty501

9 McKenna A, Hanna M, Banks E *et al.* The genome analysis toolkit: A mapreduce framework for analyzing next-generation dna sequencing data. *Genome Research* 2010;**20**:1297–303. doi:10.1101/gr.107524.110

10 Nielsen TO, Parker JS, Leung S *et al.* A comparison of PAM50 intrinsic subtyping with immunohistochemistry and clinical prognostic factors in tamoxifen-treated estrogen receptorPositive breast cancer. *Clinical Cancer Research* 2010;**16**:5222–32. doi:10.1158/1078-0432.ccr-10-1282

11 Chae YK, Chang S, Ko T *et al.* Epithelial-mesenchymal transition (EMT) signature is inversely associated with t-cell infiltration in non-small cell lung cancer (NSCLC). *Scientific Reports* 2018;**8**. doi:10.1038/s41598-018-21061-1

12 Ramaswamy S, Ross KN, Lander ES *et al.* A molecular signature of metastasis in primary solid tumors. *Nature Genetics* 2002;**33**:49–54. doi:10.1038/ng1060

13 Chang WH, Lai AG. Transcriptional landscape of DNA repair genes underpins a pan-cancer prognostic signature associated with cell cycle dysregulation and tumor hypoxia. *DNA Repair* 2019;**78**:142–53. doi:10.1016/j.dnarep.2019.04.008

14 Damotte D, Warren S, Arrondeau J *et al.* The tumor inflammation signature (TIS) is associated with anti-PD-1 treatment benefit in the CERTIM pan-cancer cohort. *Journal of Translational Medicine* 2019;**17**. doi:10.1186/s12967-019-2100-3

Transcriptomic-dependent *Fn/Fusobacteriales* impact.

15 Rooney MS, Shukla SA, Wu CJ *et al.* Molecular and genetic properties of tumors associated with local immune cytolytic activity. *Cell* 2015;**160**:48–61. doi:10.1016/j.cell.2014.12.033

16 Higgs BW, Morehouse CA, Streicher K *et al.* Interferon gamma messenger RNA signature in tumor biopsies predicts outcomes in patients with nonSmall cell lung carcinoma or urothelial cancer treated with durvalumab. *Clinical Cancer Research* 2018;**24**:3857–66. doi:10.1158/1078-0432.ccr-17-3451

17 Wang S, Song R, Wang Z *et al.* S100A8/a9 in inflammation. *Frontiers in Immunology* 2018;**9**. doi:10.3389/fimmu.2018.01298

18 Kim N, Kim HK, Lee K *et al.* Single-cell RNA sequencing demonstrates the molecular and cellular reprogramming of metastatic lung adenocarcinoma. *Nature Communications* 2020;**11**. doi:10.1038/s41467-020-16164-1

19 Becht E, Giraldo NA, Lacroix L *et al.* Estimating the population abundance of tissue-infiltrating immune and stromal cell populations using gene expression. *Genome Biology* 2016;**17**:218. doi:10.1186/s13059-016-1070-5

20 Finotello F, Mayer C, Plattner C *et al.* Molecular and pharmacological modulators of the tumor immune contexture revealed by deconvolution of RNA-seq data. *Genome Medicine* 2019;**11**. doi:10.1186/s13073-019-0638-6

21 Guinney J, Dienstmann R, Wang X *et al.* The consensus molecular subtypes of colorectal cancer. *Nature Medicine* 2015;**21**:1350–6. doi:10.1038/nm.3967

22 Isella C, Brundu F, Bellomo SE *et al.* Selective analysis of cancer-cell intrinsic transcriptional traits defines novel clinically relevant subtypes of colorectal cancer. *Nature Communications* 2017;**8**:15107. doi:10.1038/ncomms15107

23 Thorsson V, Gibbs DL, Brown SD *et al.* The Immune Landscape of Cancer. *Immunity* 2018;**48**:812–830.e14. doi:10.1016/j.immuni.2018.03.023

24 Bonneville R, Krook MA, Kautto EA *et al.* Landscape of microsatellite instability across 39 cancer types. *JCO Precision Oncology* 2017;1–15. doi:10.1200/po.17.00073

25 Mayakonda A, Lin D-C, Assenov Y *et al.* Maftools: Efficient and comprehensive analysis of somatic variants in cancer. *Genome Research* 2018;**28**:1747–56. doi:10.1101/gr.239244.118

26 Mermel CH, Schumacher SE, Hill B *et al.* GISTIC2.0 facilitates sensitive and confident localization of the targets of focal somatic copy-number alteration in human cancers. *Genome Biology* 2011;**12**. doi:10.1186/gb-2011-12-4-r41

27 Nilsen G, Liestøl K, Loo PV *et al.* Copynumber: Efficient algorithms for single- and multi-track copy number segmentation. *BMC Genomics* 2012;**13**:591. doi:10.1186/1471-2164-13-591

28 Vallat R. Pingouin: Statistics in python. *Journal of Open Source Software* 2018;**3**:1026. doi:10.21105/joss.01026

29 Fang Z. GSEApy: Gene set enrichment analysis in python. 2020. doi:10.5281/ZENODO.3748085

30 Chen EY, Tan CM, Kou Y *et al.* Enrichr: Interactive and collaborative HTML5 gene list enrichment analysis tool. *BMC Bioinformatics* 2013;**14**:128. doi:10.1186/1471-2105-14-128

Transcriptomic-dependent *Fn/Fusobacteriales* impact.

31 Kuleshov MV, Jones MR, Rouillard AD *et al.* Enrichr: A comprehensive gene set enrichment analysis web server 2016 update. *Nucleic Acids Research* 2016;**44**:W90–7. doi:10.1093/nar/gkw377

32 Hunter JD. Matplotlib: A 2D graphics environment. *Computing in science & engineering* 2007;**9**:90–5.

33 Waskom M. Seaborn: Statistical data visualization. *Journal of Open Source Software* 2021;**6**:3021. doi:10.21105/joss.03021

34 Davidson-Pilon C. Lifelines: Survival analysis in python. *Journal of Open Source Software* 2019;**4**:1317. doi:10.21105/joss.01317

35 R Core Team. *R: A language and environment for statistical computing*. Vienna, Austria:: R Foundation for Statistical Computing 2020. https://www.R-project.org/

36 Van Rossum G, Drake FL. *Python 3 reference manual*. Scotts Valley, CA:: CreateSpace 2009.

37 McKinney W, others. Data structures for statistical computing in python. In: *Proceedings of the 9th python in science conference*. Austin, TX 2010. 51–6.

38 Oliphant TE. *A guide to numpy*. Trelgol Publishing USA 2006.

39 Pedregosa F, Varoquaux G, Gramfort A *et al.* Scikit-learn: Machine learning in Python. *Journal of Machine Learning Research* 2011;**12**:2825–30.

40 Ellson J, Gansner E, Koutsofios L *et al.* Graphviz — open source graph drawing tools. In: *Lecture notes in computer science*. Springer-Verlag 2001. 483–4.

Transcriptomic-dependent *Fn/Fusobacteriales* impact.

41 Alexander Lex HS Nils Gehlenborg. UpSet: Visualization of intersecting sets. *IEEE transactions on visualization and computer graphics* 2014;**20**:1983–92. doi:10.1109/TVCG.2014.2346248

42 Seabold S, Perktold J. Statsmodels: Econometric and statistical modeling with python. In: *9th python in science conference*. 2010.